A Section 508–conformant HTML version of this article is available at https://doi.org/10.1289/EHP6990.

Use of Shotgun Metagenomics and Metabolomics to Evaluate the Impact of Glyphosate or Roundup MON 52276 on the Gut Microbiota and Serum Metabolome of Sprague-Dawley Rats

Robin Mesnage,[1] Maxime Teixeira,[2] Daniele Mandrioli,[3] Laura Falcioni,[3] Quinten Raymond Ducarmon,[4] Romy Daniëlle Zwittink,[4] Francesca Mazzacuva,[5] Anna Caldwell,[5] John Halket,[5] Caroline Amiel,[2] Jean-Michel Panoff,[2] Fiorella Belpoggi,[3] and Michael Nicolas Antoniou[1]

[1]Gene Expression and Therapy Group, Department of Medical and Molecular Genetics, King's College London, Faculty of Life Sciences & Medicine, Guy's Hospital, London, UK
[2]Unité de Recherche Aliments Bioprocédés Toxicologie Environnements, University of Caen Normandy, Caen, France
[3]Ramazzini Institute, Bologna, Italy
[4]Center for Microbiome Analyses and Therapeutics, Leiden University Medical Center, Leiden, Netherlands
[5]Mass Spectrometry Facility, King's College London, London, UK

Background: There is intense debate on whether glyphosate can inhibit the shikimate pathway of gastrointestinal microorganisms, with potential health implications.

Objectives: We tested whether glyphosate or its representative EU herbicide formulation Roundup MON 52276 affects the rat gut microbiome.

Methods: We combined cecal microbiome shotgun metagenomics with serum and cecum metabolomics to assess the effects of glyphosate [0.5, 50, 175 mg/kg body weight (BW) per day] or MON 52276 at the same glyphosate-equivalent doses, in a 90-d toxicity test in rats.

Results: Glyphosate and MON 52276 treatment resulted in ceca accumulation of shikimic acid and 3-dehydroshikimic acid, suggesting inhibition of 5-enolpyruvylshikimate-3-phosphate synthase of the shikimate pathway in the gut microbiome. Cysteinylglycine, γ-glutamylglutamine, and valylglycine levels were elevated in the cecal microbiome following glyphosate and MON 52276 treatments. Altered cecum metabolites were not differentially expressed in serum, suggesting that the glyphosate and MON 52276 impact on gut microbial metabolism had limited consequences on physiological biochemistry. Serum metabolites differentially expressed with glyphosate treatment were associated with nicotinamide, branched-chain amino acid, methionine, cysteine, and taurine metabolism, indicative of a response to oxidative stress. MON 52276 had similar, but more pronounced, effects than glyphosate on the serum metabolome. Shotgun metagenomics of the cecum showed that treatment with glyphosate and MON 52276 resulted in higher levels of *Eggerthella* spp., *Shinella zoogleoides*, *Acinetobacter johnsonii*, and *Akkermansia muciniphila*. *Shinella zoogleoides* was higher only with MON 52276 exposure. *In vitro* culture assays with *Lacticaseibacillus rhamnosus* strains showed that Roundup GT plus inhibited growth at concentrations at which MON 52276 and glyphosate had no effect.

Discussion: Our study highlights the power of multi-omics approaches to investigate the toxic effects of pesticides. Multi-omics revealed that glyphosate and MON 52276 inhibited the shikimate pathway in the rat gut microbiome. Our findings could be used to develop biomarkers for epidemiological studies aimed at evaluating the effects of glyphosate herbicides on humans. https://doi.org/10.1289/EHP6990

Introduction

The gastrointestinal (GI) tract is colonized by a large collection of microorganisms, including bacteria, archaea, fungi, viruses, and small eukaryotes. Bacteria are physically separated from the gut epithelial lining by the inner mucus layer, which prevents epithelial colonization and, potentially, enteric infection (Ducarmon et al. 2019). The gut microbiome metabolism of dietary components, environmental chemicals, and pharmaceuticals has a major influence on health (Koppel et al. 2017). Given that the effects of toxic chemicals on the gut microbiome are not systematically tested in the battery of premarket tests, concerns have been raised about the potential impacts of environmental contaminants, such as glyphosate (Tsiaoussis et al. 2019).

Glyphosate is the world's most used herbicide ingredient (Benbrook 2016) and is one of the most frequently detected pesticide residues in foodstuffs (EFSA 2017). This is due to the fact that it is frequently sprayed on crops (especially cereals such as oats and wheat) to accelerate ripening and facilitate harvest or to clear weeds in the cultivation of glyphosate-tolerant genetically modified crops (Benbrook 2016; EFSA 2017).

The primary mechanism by which glyphosate acts as a herbicide is by inhibiting the enzyme 5-enolpyruvylshikimate-3-phosphate synthase (EPSPS) of the shikimate pathway, which is responsible for aromatic amino acid biosynthesis (Schönbrunn et al. 2001). The mode of action of glyphosate on EPSPS is to compete with phosphoenolpyruvate, which is condensed with shikimate-3-phosphate to form EPSP. The action of EPSPS is the penultimate step in the seven-step shikimate pathway (Figure 1) leading to the biosynthesis of chorismate (Knaggs 2001). Although it is generally considered that the inhibition of aromatic amino acid synthesis is the main outcome of glyphosate's effects on the shikimate pathway, chorismate is also a precursor for the biosynthesis of secondary metabolites, including ubiquinone, menaquinone, lignans, tannins, and flavonoids (Knaggs 2001).

Given that the shikimate pathway is absent in animal cells, including humans, glyphosate has been asserted to have a high safety profile. However, the shikimate pathway also exists in some microorganisms (Knaggs 2001). Because this pathway is essential for the viability of some pathogenic microorganisms, such as *Mycobacterium tuberculosis* (Parish and Stoker 2002), or

Address correspondence to Michael Nicolas Antoniou, Department of Medical and Molecular Genetics, 8th Floor, Tower Wing, Guy's Hospital, Great Maze Pond, London SE1 9RT, UK. Telephone: 44 (0)20 7848 8501. Email: michael.antoniou@kcl.ac.uk

Supplemental Material is available online (https://doi.org/10.1289/EHP6990).

R.M. has served as a consultant on glyphosate risk assessment issues as part of litigation in the United States over glyphosate health effects. All other authors declare they have no actual or potential competing financial interests.

Received 28 February 2020; Revised 10 December 2020; Accepted 11 December 2020; Published 27 January 2021.

Note to readers with disabilities: *EHP* strives to ensure that all journal content is accessible to all readers. However, some figures and Supplemental Material published in *EHP* articles may not conform to 508 standards due to the complexity of the information being presented. If you need assistance accessing journal content, please contact ehponline@niehs.nih.gov. Our staff will work with you to assess and meet your accessibility needs within 3 working days.

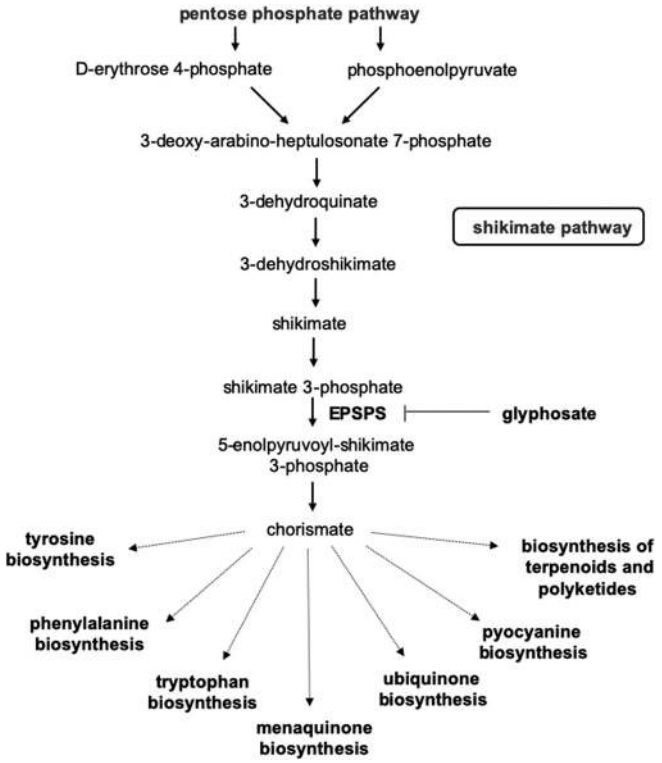

Figure 1. The shikimate pathway and its associated biosynthesis pathways. Information about the biosynthetic pathway associated with the shikimate pathways metabolites were retrieved from the KEGG Orthology database. Note: EPSPS, enolpyruvylshikimate-3-phosphate synthase; KEGG, Kyoto Encyclopedia of Genes and Genomes.

unicellular parasites, such as the malaria parasite *Plasmodium falciparum* (McConkey et al. 1994; Roberts et al. 1998), shikimate-pathway enzymes are targets for the creation of antibiotics, as well as antifungal and antiparasitic drugs (Coggins et al. 2003). It has been found that glyphosate in combination with dicarboxylic acids (for example, oxalate) acts as an antiparasitic agent and can potentially be used to treat infections caused by protozoan parasites, such as *Toxoplasma gondii, Plasmodium falciparum*, and *Cryptosporidium parvum* (Abraham 2010).

Glyphosate is primarily excreted in the feces, which makes the GI tract the biological compartment exposed to the highest concentrations of this compound (Brewster et al. 1991). It is still unclear whether glyphosate is metabolized by the gut microbiome (Zhan et al. 2018). The main metabolite of glyphosate is aminomethylphosphonic acid, which can be generated by some soil microorganisms through the glycine oxidase pathway or by oxidation of the glyphosate carbon–phosphorus (C-P) bond (Barrett and McBride 2005). Another biochemical pathway found in some soil microorganisms is the C-P lyase pathway, also called the sarcosine pathway, which cleaves the glyphosate C-P bond to phosphate and sarcosine (Hove-Jensen et al. 2014). A study of publicly available gut metagenomes also suggests that glyphosate might be degraded by some Proteobacteria in the human gut microbiome using the C-P lyase pathway (Mesnage and Antoniou 2020).

It has been hypothesized that glyphosate may contribute to the development and progression of various human diseases by generating a selection pressure on some microbial communities in the human gut microbiome (Mesnage and Antoniou 2017). Some authors have proposed that the action of glyphosate on the gut microbiome can be linked with the rise in nonceliac gluten sensitivity and the large rise in the incidence of autism spectrum disorders in children within the United States (Samsel and Seneff 2013). However, this remains unsubstantiated by experimental evidence (Mesnage and Antoniou 2017). Although some studies have investigated the effects of glyphosate on the gut microbiome in rats (Lozano et al. 2018; Mao et al. 2018; Nielsen et al. 2018), cows (Riede et al. 2016), pigs (Krause et al. 2020), honey bees (Motta et al. 2018), and turtles (Kittle et al. 2018), there is still intense debate as to whether glyphosate's interference with the shikimate pathway in microorganisms inhabiting the human GI tract can be a source of negative health outcomes.

To address this knowledge gap in glyphosate toxicology, we used a multi-omics strategy combining cecal microbiome shotgun metagenomics with serum and cecum metabolomics to test whether the impact of glyphosate, or its representative EU commercial herbicide formulation Roundup MON 52276, on gut microbial metabolism has an effect on the microbiome–host interface. We took advantage of recent progress in high-throughput omics technologies, which have been used to evaluate molecular composition (Taylor et al. 2018) and to predict chemical mode of action in bacteria (Zampieri et al. 2018). Metabolomics is increasingly used to understand the function of the gut microbiome (e.g., Zierer et al. 2018). Combined with shotgun metagenomics sequencing techniques to identify and quantify the whole genomes from a larger range of microorganisms (bacteria, fungi, viruses and protists), we captured the modifications of the metabolic activity of the gut microbiome after exposure to glyphosate or MON 52276.

Material and Methods

Experimental Animals

The experiment was conducted on young adult female Sprague-Dawley rats (8 wk of age at the start of treatment), in accordance with Italian law regulating the use and humane treatment of animals for scientific purposes (Government of Italy 2014). Before commencing the experiment, the protocol was examined by the animal welfare body for approval. The protocol of the experiment was authorized by the ad hoc commission of the Italian Ministry of Health (authorization no. 447/2018-PR).

Female Sprague-Dawley rats were generated in-house at the Cesare Maltoni Cancer Research Center, Ramazzini Institute, following an outbreeding program, and were subjected to ear-punch marking using the Jackson Laboratory system for the purposes of identification. Female animals were chosen to make our results comparable to our previous studies, in which we showed that the long-term exposure to Roundup GT plus (GT^+) was associated with the development of fatty liver disease (Mesnage et al. 2015, 2017). Animals were randomized after weaning in order to have at most one sister per litter in each group. Homogeneous body weight (BW) within the different groups was also ensured. Animals of 6 wk of age were acclimatized for 2 wk before the start of the experiment. Rats were housed in polycarbonate cages ($41 \times 25 \times 18$ cm) with stainless steel wire tops and a shallow layer of white wood shavings as bedding. The animals were housed in the same room, three per cage, maintained at a temperature of $22°C \pm 3°C$ and relative humidity of $50\% \pm 20\%$. Artificial lighting was provided on a 12-h light/dark cycle. The cages were periodically rotated on their racks to minimize effects due to cage position on animals.

Treatments

Seven groups of 12 female Sprague-Dawley rats of 8 wk of age were treated for 90 d (Excel Table S1). They received *ad libitum* a rodent diet supplied by SAFE. The feed was analyzed to identify possible contaminants or impurities by Eurofins and the Institut

Scientifique d'Hygiène et d'Analyze (see the file "File Contaminant Screening"). Nutrients, pesticides, dioxins, mycotoxins, isoflavones, heavy metals, and polychlorinated biphenyls, as well as some microorganisms, were measured. Glyphosate was not detected (limit of quantification: 0.01 mg/kg). The only pesticide residue detected was piperonyl butoxide, which was found at a concentration of 0.034 ± 0.017 mg/kg. Glyphosate and MON 52276 (at the same glyphosate-equivalent dose) were administered via drinking water to give a daily intake of 0.5, 50, and 175 mg/kg BW per day, which respectively represent the EU acceptable daily intake (ADI), the EU no observed adverse effect level (NOAEL) and the U.S. NOAEL (EFSA 2015; U.S. EPA 2002). Glyphosate was purchased from Merck KGaA (Sigma Aldrich) with purity $\geq 95\%$. MON 52276 was sourced from the Italian market as Roundup Bioflow (commercial name). MON 52276 is the formulated glyphosate-based herbicide used for the EU's review for market registration, and it is sold under different trade names in Europe (Roundup Pro Biactive in Ireland, Roundup Extra 360 or Roundup Star 360 in France, Roundup BioFlow in Italy, Roundup Ultra in Belgium and Austria, or Roundup Bio in Finland) (Mesnage et al. 2019). Tap water from the local water supplier was administered in glass bottles *ad libitum*. Drinking water was discarded and the bottles were cleaned and refilled daily. The doses of MON 52276 and glyphosate for experimental groups were calculated every week based on weekly mean BWs and weekly mean water consumption in order to achieve the desired dosage, considering that MON 52276 contains 360 g/L of glyphosate.

Clinical Observations

Animals were checked for general status three times a day from Monday to Saturday and twice on Sundays. Status, behavior, and clinical parameters of experimental animals were checked weekly, starting from 2 wk before the start of the treatments until the end of the experiment (13 wk of treatment). The daily water (Excel Table S2) and food consumption (Excel Table S3) per cage were measured before the start of the experiment and then weekly for the entire 13-wk duration of the treatment. The day before sacrifice, the animals were allocated into metabolic cages (model 3701M081; Tecniplast spa Italy). After approximately 16 h in a metabolic cage, total water consumption was registered for each animal. Animals remained in metabolic cages until sacrifice. The BW of the experimental animals was measured before the start of the treatment and then weekly for 13 wk (Excel Table S4). Before sacrifice, the animals were anesthetized by inhalation using a mixture of carbon dioxide and oxygen (70% and 30%, respectively), and about 7.5 mL of blood was collected from the vena cava. The blood in its collection tube was stored at room temperature for 20 min and then centrifuged at 3,000 rpm for 10 min to obtain serum, which was aliquoted into labeled cryovials and stored at -70°C. At the time of sacrifice, two vials of 100-mg cecal content were collected to perform the gut microbiome evaluation (one for the shotgun metagenomics and one for the metabolomics). The sampling schedule is detailed in Table S1.

Metabolomics Analysis

Metabolon Inc. (Durham, NC) was contracted to conduct the metabolomics analysis. Serum and fecal samples were prepared using the automated MicroLab STAR system from the Hamilton Company. The samples were first lyophilized and then weighed. Between 20 and 30 mg of dried sample was then used for the analysis. The samples were prepared by adding water at a 50:1 vol:wt ratio and homogenized via agitation in the presence of steel beads in a Genogrinder (GenoGrinder 2000; Gen Mills). In order to ensure that a consistent amount of sample was analyzed, an equal aliquot of the resulting homogenized material was used for metabolite extraction from each of the samples. Proteins were precipitated with methanol (500 µL of methanol added to 100 µL of sample) under vigorous shaking for 2 min (using the GenoGrinder 2000). Following the precipitation step, the samples were centrifuged for 10 min at $680 \times g$ to pellet the precipitated material, and the supernatant was transferred to analytical plates as previously described (Ford et al. 2020). Samples were placed briefly in a TurboVap (Zymark) to remove the organic solvent. The sample extracts were stored overnight under nitrogen before preparation for analysis. The resulting extract was analyzed on four independent instrument platforms: two different separate reverse phase ultra-high performance liquid chromatography–tandem mass spectroscopy analysis (RP/UPLC-MS/MS) with positive ion mode electrospray ionization (ESI), a RP/UPLC-MS/MS with negative ion mode ESI, as well as a by hydrophilic-interaction chromatography (HILIC)/UPLC-MS/MS with negative ion mode ESI.

All UPLC-MS/MS methods used a Waters ACQUITY UPLC and a Thermo Scientific Q-Exactive high-resolution/accurate mass spectrometer interfaced with a heated ESI source and Orbitrap mass analyzer operated at 35,000 mass resolution. The sample extract was dried and then reconstituted in solvents compatible to each of the four methods used. The details of the solvents and chromatography used are described by Ford et al. (2020). Each reconstitution solvent contained a series of isotopically labeled or halogenated standards at fixed concentrations (Ford et al. 2020) to ensure injection and chromatographic consistency. One aliquot was analyzed using acidic positive ion conditions, which are optimized for more hydrophilic compounds. In this method (LC/MS/MS positive polar; see Ford et al. 2020), the extract was gradient eluted from a C18 column (Waters UPLC BEH C18-2.1×100 mm, 1.7 µm) using water and methanol, containing 0.05% perfluoropentanoic acid (PFPA) and 0.1% formic acid (FA) at pH ~ 2.5 at a flow rate of 0.35 mL/min. Gradient elution time was 3.35 min. Another aliquot was also analyzed using acidic positive ion conditions, chromatographically optimized for more hydrophobic compounds. In this method (LC/MS/MS positive lipid; see Ford et al. 2020), the extract was gradient eluted from the same aforementioned C18 column using methanol, acetonitrile, water, 0.05% PFPA, and 0.01% FA and was operated at an overall higher organic content at a flow rate of 0.60 mL/min. Another aliquot was analyzed using basic negative ion optimized conditions using a separate dedicated C18 column (LC/MS/MS Neg; as described by Ford et al. 2020). The basic extracts were gradient eluted from the column using methanol and water, with 6.5 mM ammonium bicarbonate at pH 8. The gradient was linear from 0.5% to 70% mobile phase containing 95% methanol and 5% water over 4.0 min, and then rapid to 99% (same mobile phase) in 0.5 min. The flow rate was 0.35 mL/min. The fourth aliquot (method LC/MS/MS Polar) was analyzed via negative ionization following elution from a HILIC column (Waters UPLC BEH Amide 2.1×150 mm, 1.7 µm) using a gradient consisting of water and acetonitrile with 10 mM ammonium formate, pH 10.8. Flow rate was 0.50 mL/min. The MS analysis alternated between MS and data-dependent MS^n scans using dynamic exclusion. The scan range covered 70–1,000 m/z. A total of 749 and 744 compounds were detected in serum (Excel Table S5) and cecum (Excel Table S6), respectively.

The raw data were extracted, peak-identified, and quality control (QC) processed using Metabolon's hardware and software as previously described (DeHaven et al. 2010). Serum and cecum metabolites were identified by comparison with libraries of authenticated standards with known retention time/indices, mass to charge ratios, and chromatographic and MS/MS spectral data. Identification was based on retention index, mass match

(±10 ppm), and forward- or reverse-search matching between the experimental data and library standards. More than 3,300 purified standard compounds were registered into the laboratory information management system. The database server is run with Oracle 10.2.0.1 Enterprise Edition. Several controls were analyzed in concert with the experimental samples (Figure S1; Tables S2 and S3) and were used to calculate instrument variability and overall process variability (Table S4). Experimental samples were randomized across the platform run with QC samples spaced evenly among the injections, as outlined in Figure S1. Peak area values allowed the determination of relative quantification among samples (Evans et al. 2009). Absolute quantifications including the determination of limits of detection would require the optimization and validation of compound-specific assays. The raw data is available in Metabolights, with the accession number MTBLS138 (https://www.ebi.ac.uk/metabolights/MTBLS138).

Shikimic Acid Quantification by HPLC-MS/MS

The experimental protocol used to quantify shikimic acid in serum was based on a published method (Noh et al. 2020). Shikimic acid was quantified by HPLC-MS/MS with a Thermo Scientific Quantum Access mass spectrometer with a Thermo Accela LC pump and CTC autosampler. Diclofenac was used as an internal standard. The substances were separated on a C18 Thermo Scientific Accucore HPLC column (100 × 2.1 mm, 2.6 µm). The elution rate was 0.2 mL/min and run time was 10 min. Retention times for shikimic acid and diclofenac were 1.5 min and 5.9 min, respectively. For the mass spectrometry, negative ion mode ESI was used. Spray voltage was maintained at 4,000 V and 350°C. Selected reaction monitoring (SRM) transitions (Table S5) were determined from infusion data acquired in central mode data type and with a peak width of 0.4 m/z.

Protein precipitation was achieved by mixing 100 µL serum with 500 µL acetonitrile and 50 µL internal standard, followed by vortexing. Samples were then centrifuged 5 min at 14,000 rpm. The resulting supernatants were evaporated to dryness in a rotavap at 30°C. This extract was then reconstituted in 80 µL acetonitrile:water and centrifuged 5 min at 14,000 rpm before being transferred to injection vials.

Shotgun Metagenomics

DNA was extracted from 100 mg of cecum content using the Quick-DNA Fecal/Soil Microbe Miniprep Kit (ZymoResearch) with minor adaptations from the manufacturer's instructions. Adaptations were as follows: bead beating was performed at 5.5 m/s three times for 60 s (Precellys 24 homogenizer; Bertin Instruments), and 2.50 µL of an elution buffer was used to elute the DNA, following which, the eluate was run over the column once more to increase DNA yield. One negative control (no sample added) and one positive control (ZymoBIOMICS Microbial Community Standard; ZymoResearch) were taken along during the DNA extraction procedures and subsequently sequenced. DNA was quantified using the Qubit HS dsDNA Assay kit on a Qubit 4 fluorometer (Thermo Fisher Scientific).

Shotgun metagenomics was performed under contract by GenomeScan. The NEBNext Ultra II FS DNA module (catalog # NEB #E7810S/L) and the NEBNext Ultra II Ligation module (catalog # NEB #E7595S/L) were used to process the samples. Fragmentation, A-tailing, and ligation of sequencing adapters of the resulting product was performed according to the procedure described in the NEBNext Ultra II FS DNA module and NEBNext Ultra II Ligation module instruction manual. Quality and yield after sample preparation was measured using the fragment analyzer. The size of the resulting product was consistent

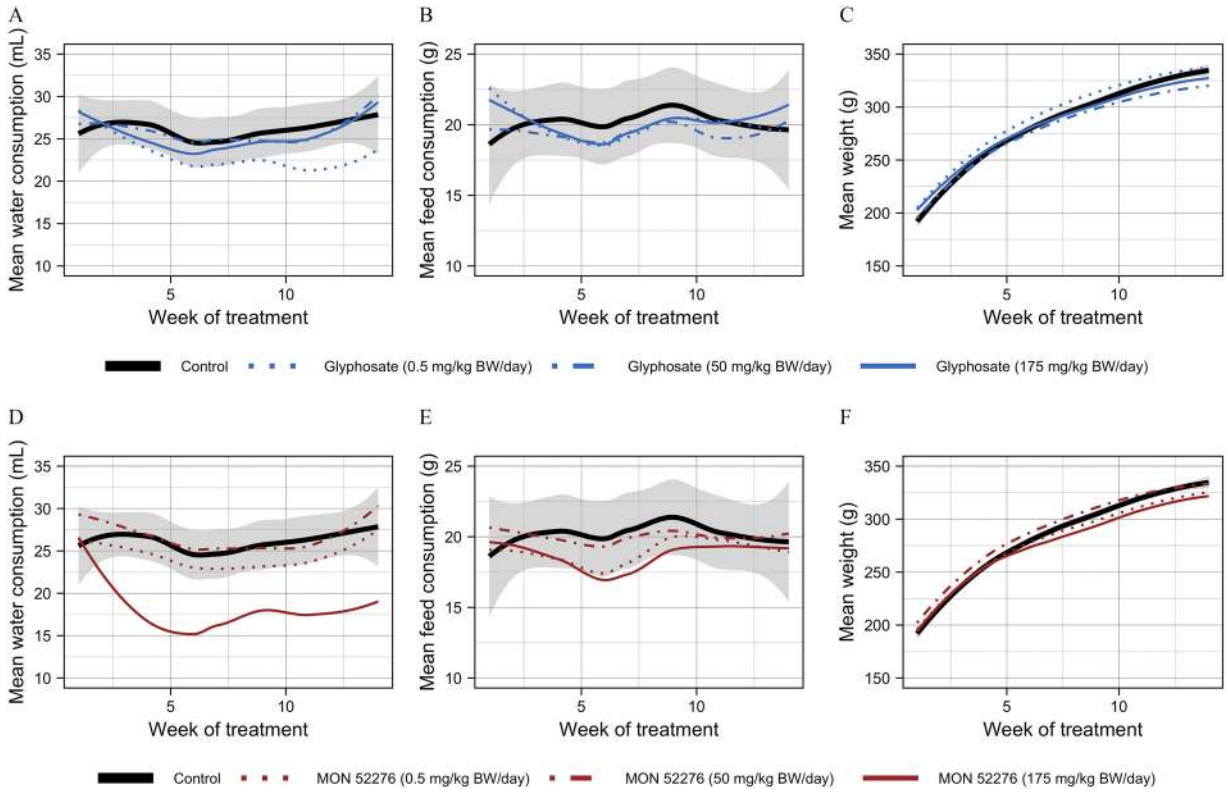

Figure 2. Changes in water consumption, food consumption, and body weight are shown for adult female Sprague-Dawley rats administered with (A–C) glyphosate and (D–F) Roundup MON 52276 in drinking water for 90 d. Curves are smoothed conditional means of weekly body weight and food and water intake measurements. $n = 12$ per group. The gray shading is the 95% confidence interval for the control group. Note: BW, body weight.

Table 1. OPLS-DA models of the metabolomics of the host-gut microbiota in Sprague-Dawley rats exposed to glyphosate and Roundup MON 52276. Female rats were administered via drinking water to 0.5, 50, and 175 mg/kg BW per day glyphosate and MON 52276 at a glyphosate-equivalent dose for 90 days.

Metabolome	OPLS-DA	Gly_0.5	Gly_50	Gly_175	Mon_0.5	Mon_50	Mon_175
Cecum	R2Y	0.63	0.65	0.99	0.51	0.71	0.99
Cecum	Q2	0.06	0.16*	0.44*	0.24*	0.53*	0.54*
Serum	R2Y	0.67	0.71	0.76	0.83	0.91	0.89
Serum	Q2	0.2	0.31*	0.22	0.49**	0.52**	0.4**

Note: The predictive ability (Q2) and the percentage of the variance of class variables (R2Y) from these OPLS-DA are presented along the *p*-value of a 1,000-time permutation test showing when the predictive ability of the model (Q2) is not part of the distribution formed by the statistic from the permuted data. $n = 10$ per group. Doses: 0.5, 50, and 175 mg/kg BW per day of glyphosate (Gly_0.5; Gly_50; Gly_175) or MON 52276 (Mon_0.5; Mon_50; Mon_175). BW, body weight; OPLS-DA, orthogonal partial least squares discriminant analysis. *, $pQ2 < 0.05$; **, $pQ2p < 0.01$).

with the expected size of ~500–700 bp. Clustering and DNA sequencing using the NovaSeq6000 was performed according to the manufacturer's protocols. A concentration of 1.1 nM of DNA was used. NovaSeq control software NCS (version 1.6) was used.

Shotgun metagenomics data sets were analyzed with Rosalind, the Biomedical Research Centre/King's College London high-performance computing cluster. First, data were preprocessed using the software package preprocessing (version 0.2.2; https://anaconda.org/fasnicar/preprocessing). In brief, this package concatenates all forward reads into one file and all reverse reads into another file; then uses trim_galore to remove Illumina adapters, trim low-quality positions and unknown positions (UNs), and discard low-quality (i.e., quality <20 or >2 Ns) or too-short reads (<75 bp); removes contaminants (phiX and rat genome sequences); and ultimately sorts and splits the reads into R1, R2, and UN sets of reads. After preprocessing, a total of 20.7 ± 4.9 million paired-end non-rat cleaned reads remained. The raw data are available from the National Center for Biotechnology Information (NCBI), with BioProject accession no. PRJNA609596 (https://www.ncbi.nlm.nih.gov/bioproject/PRJNA609596).

Given that there is no gold standard for the computational analyses of shotgun metagenomics, we used a combination of approaches. In order to use as many DNA reads as possible, we inferred the taxonomy with the NCBI Reference Sequence (RefSeq) database on the metagenomics Rapid Annotations using Subsystems Technology (RAST) server (Keegan et al. 2016). The taxonomy of 55% of our non-rat cleaned reads was assigned (Excel Table S7). Given that the amplification of 16S rRNA gene sequences was frequently used to assign taxonomy in previous glyphosate gut microbiome studies, we also isolated 16S rRNA gene reads from the shotgun metagenomics data sets, using the metagenomics RAST server with a cutoff of 70% identity to ribosomal sequences from a reduced version of M5RNA with SortMeRNA (Kopylova et al. 2012). An average of 20,000 reads per sample was mapped to 16S rRNA genes, and the taxonomy was assigned using the SILVA database (Excel Table S8). We also inferred the taxonomy with IGGsearch (iggdb_v1.0.0_gut database), which uses taxa-specific marker genes (Excel Table S9) and circumvents problems associated with the amplification of single amplicons, such as in the case of the 16S rRNA gene (Nayfach et al. 2019). In order to understand changes in cecum microbiome functional potential, we used a bacterial gene catalog from the Sprague-Dawley rat gut microbiome using Bowtie2 (version 2.2.5; Pan et al. 2018). A total of 23.5 ± 6.8% of the reads aligned to this catalog. Count data were then extracted from the Binary Alignment Map files using SAMtools (version 1.4; Li et al. 2009). Approximately 41% of the mapped reads were assigned with a Kyoto Encyclopedia of Genes and Genomes (KEGG) Orthology annotation (Excel Table S10). However, this was not used to infer the taxonomy, given that 90.6% of the contigs detected in our metagenome data sets were not annotated at the species level defined by Pan et al. (2018). ShortBRED was also used to quantify the abundance of the EPSPS enzyme (Excel Table S11) with default parameters (Kaminski et al. 2015). For this purpose, a set of markers specific to EPSPS enzymes was created from InterPro family IPR006264 (3-phosphoshikimate 1-carboxyvinyltransferase) with UniRef90 as the reference database using ShortBRED-Identify. ShortBRED-Quantify was then used to measure the abundance of EPSPS markers in the shotgun metagenomic sequence reads with default parameters (Excel Table S11).

In Vitro *Study of Bacterial Growth*

A stock solution of 5.6 g/L glyphosate was made in water and used to inoculate a freshly prepared de Man, Rogosa, and Sharpe (MRS) broth without peptone (Table S6). Roundup GT$^+$ and MON 52276 at 450 g/L and 360 g/L respectively, were directly diluted in bacterial broth. *Lacticaseibacillus rhamnosus* (formerly known as *Lactobacillus rhamnosus*) (Zheng et al. 2020) strains were provided by the Université de Caen Microbiologie Alimentaire culture collection, identification nos. 2927 (LB2), 2929 (LB3), 2933 (LB5), and 5164 (LB7). Three of these strains have their reference sequences (LB2 = CIP A158; LB3 = CIP 71.38; LB5 = CIP 103888) in the biobank of the Center de Ressources Biologiques Institut Pasteur (Paris, France), while the strain LB7 was described by Henri-Dubernet et al. (2008). These strains were used because *Lacticaseibacillus rhamnosus* is prevalent in the human gut and has relevant health-promoting properties as a probiotic (Capurso 2019) and also because previous rat studies investigating the effects of glyphosate on the gut microbiome suggested that Lactobacilli are the most affected bacteria (Lozano et al. 2018; Mao et al. 2018). The broth dilution method was used to determine how pesticides can modify bacterial growth under aerobic conditions (Wiegand et al. 2008). Bacteria from overnight cultures grown in MRS in tubes stored in a 37°C incubator were resuspended to an $OD_{600nm} = 0.3$ and further diluted 1,000-fold in MRS broth without peptone for *L. rhamnosus* to obtain approximately 10^5 CFU/mL, as confirmed in each experiment by plating the cell suspension on MRS agar plates, which were incubated aerobically at 37°C. Glyphosate was tested from concentrations one-tenth (~0.5 mg/L) those of the glyphosate dilutions in the drinking water of animals receiving the lowest experimental dose in the present study. Plates were inspected after 24 h and 48 h. All experiments were performed in triplicate.

Statistical Analysis

Statistical analysis was performed in R (version 3.6.1; R Development Core Team). Peak area values for cecum (Excel Table S12) and serum (Excel Table S13) metabolomes were median scaled and log transformed, and any missing values were imputed with sample set minimums. The metabolome data orthogonal partial least squares discriminant analysis (OPLS-DA) was performed using MetaboAnalyst (version 4.0; Chong et al. 2018). Log-transformed data were analyzed using a one-way analysis of variance (ANOVA) adjusted for multiple comparisons with the false discovery rate (FDR) procedure with R package qvalue (version

2.20.0). Tukey honest significant differences (Tukey HSD) tests were computed to determine if there was a difference in mean value between the different treatment groups. The correlations between Euclidean distances from the samples in the cecum and serum metabolome were studied using the Mantel permutation test (method: spearman) with the R package cultevo (version 1.0.2).

For the shotgun metagenomics, a compositional data analysis approach was used because gut metagenomics data sets are typically zero-inflated (Knight et al. 2012). We used ALDE × 2 (version 1.20.0) for differential (relative) abundance analysis of proportional data (Fernandes et al. 2013). Statistical analysis was performed on a data set corrected for asymmetry (uneven sequencing depths) using the interquartile log-ratio method, which identifies features with reproducible variance. We assessed statistical significance using a Kruskal-Wallis test, with *p*-values adjusted for multiple comparisons with the FDR approach.

Alpha (Shannon diversity index) was analyzed with the Vegan R package (version 2.5.6). *p*-Values for alpha diversity were computed using an ANOVA test. Beta diversity was estimated using pairwise Bray-Curtis distances among samples with the Vegan R package. *p*-Values for beta diversity were computed using permutational multivariate ANOVA tests (10,000 permutations) done using the adonis function in the Vegan package.

KEGG annotation analysis was performed using the output of the alignment to gene catalog from the Sprague-Dawley rat gut microbiome (Pan et al. 2018). Aggregated counts for each KEGG Orthology (KO) annotation were also normalized as counts per million before the statistical significance was assessed using a Kruskal-Wallis test, with *p*-values adjusted with the FDR approach.

Statistical analyses of *in vitro* tests on bacterial growth were performed using GraphPad Prism (version 8.0.1; GraphPad Software, Inc.). Differences between treatment groups at different concentrations are performed using a Kruskal-Wallis test with Dunn's multiple comparison post-test.

Results

The primary aim of the present study was to determine the effects of glyphosate on the rat gut microbiome. However, as some commercial GBH products have been shown to be more toxic than glyphosate alone because they contain other potentially toxic compounds (Mesnage et al. 2019), we deemed it important to compare the effects of glyphosate to a representative EU Roundup formulation (MON 52276) administered at the same glyphosate-equivalent dose. The doses tested were 0.5, 50, and 175 mg/kg BW per day glyphosate. These were chosen because they respectively represent the EU ADI, the EU NOAEL, and the U.S. NOAEL and are thus of regulatory relevance (EFSA 2015; U.S. EPA 2002). No significant differences were observed in water consumption (Figure 2A,D), feed consumption (Figure 2B,E), or mean BW (Figure 2C,F), except for the group administered with the highest dose of MON 52276 (175 mg/kg BW per day glyphosate-equivalent dose), which had a lower water consumption than the other groups.

Cecum Metabolomics

The metabolomics analysis detected 749 metabolites in the serum samples and 744 metabolites in the cecal content. We first evaluated the effects of glyphosate and MON 52276 using multivariate analyses. OPLS-DA revealed that treatment with both glyphosate and MON 52276 led to differences in the cecum microbiome compared with treatment with control (Table 1). The OPLS-DA was not discriminatory at the lowest dose of glyphosate tested, but it was for MON 52276.

A large number of metabolites were affected in a dose-dependent manner in the cecum metabolome (Figure 3). The levels of 14 metabolites were significantly different in rats after treatment with glyphosate or MON 52276 (Table 2) compared with rats treated with controls (FDR <0.05). The most striking effect was an accumulation of shikimate and 3-dehydroshikimate (Table 2), which are metabolites upstream of the reaction catalyzed by EPSPS in the shikimate pathway (Figure 1). These metabolites were undetectable in samples from untreated control animals.

Levels of dipeptides involved in the regulation of redox balance (prolyglycine, cysteinylglycine, valylglycine) were also significantly higher in a dose-dependent manner in MON 52276- and glyphosate-

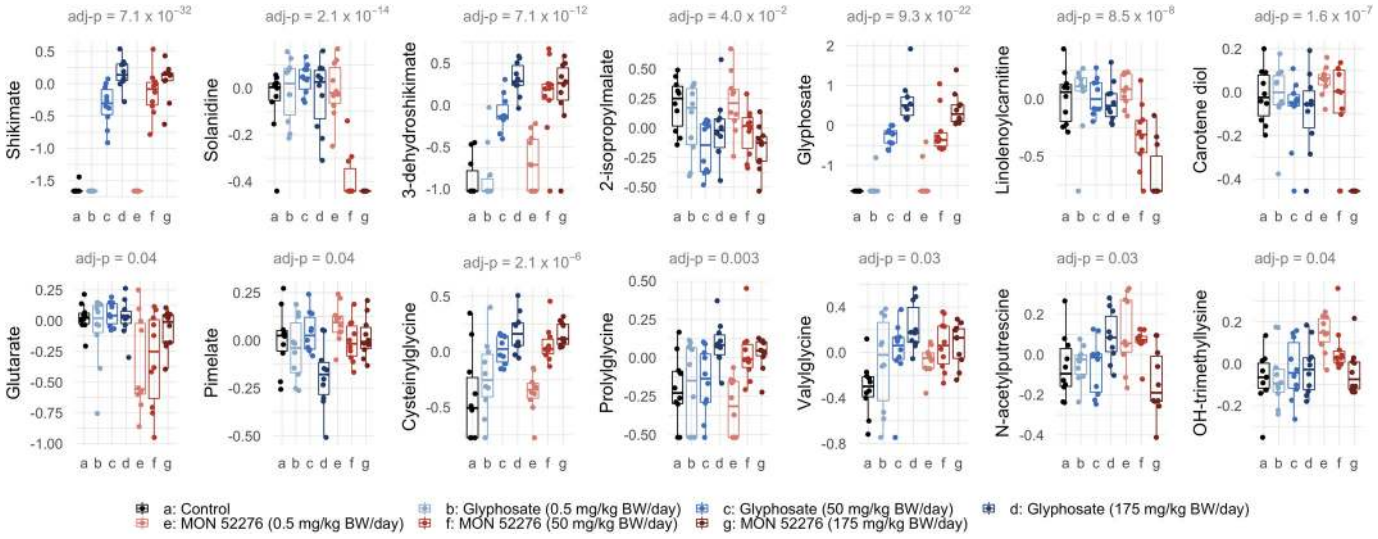

Figure 3. Differences in the level of cecum metabolites after exposure to glyphosate or Roundup MON 52276. Female Sprague-Dawley rats were administered via drinking water to 0.5, 50, and 175 mg/kg BW per day glyphosate and MON 52276 at the same glyphosate-equivalent dose for 90 d. A total of 14 metabolites had adjusted $p < 0.05$ (*adj-p*) according to an ANOVA adjusted for multiple comparisons with the FDR procedure. Log-transformed abundance values are shown as box plots with the median, two hinges (the 25th and 75th percentiles), and two whiskers extending to the furthest observation ≤1.5 times the interquartile range, along with individual values for each metabolite (solid circles). $n = 10$ per group. Note: ANOVA, analysis of variance; BW, body weight; FDR, false discovery rate.

Table 2. Cecum metabolomics of the gut microbiota in Sprague-Dawley rats exposed to glyphosate and Roundup MON 52276.

Metabolite	Pathway	Gly_0.5	Gly_50	Gly_175	Mon_0.5	Mon_50	Mon_175
Shikimate	Food component[#]	−1.1	24.7[***]	69.8[***]	−1.1	42.5[***]	55.9[***]
Solanidine	Food component[#]	1.1	1.2	1.1	1.1	−2.2[***]	−2.6[***]
3-Dehydroshikimate	Food component[#]	1.4	5.8[***]	14.5[***]	1.7	11.9[***]	12.3[***]
2-Isopropylmalate	Food component[#]	−1.3	−2.3[*]	−1.5	1.1	−1.7	−2.4[*]
Glyphosate	Chemical	1.6	25.8[***]	495.4[***]	3.2	80.9[***]	199.7[***]
Linolenoylcarnitine (C18:3)	Fatty acid metabolism[#]	1.0	−1.1	−1.2	1.1	−2.1[*]	−4.3[***]
Carotene diol	Vitamin A metabolism	1.0	−1.1	−1.1	1.2	−1.1	−2.9[***]
Glutarate	Fatty acid, dicarboxylate	−1.1	1.1	1.0	−1.7[*]	−1.7	−1.2
Pimelate	Fatty acid, dicarboxylate	−1.1	1.1	−1.5[*]	1.2	−1.1	−1.0
Cysteinylglycine	Glutathione metabolism	1.3	1.8[**]	2.7[***]	−1.3	2.1[***]	2.4[***]
Prolylglycine	Dipeptide[#]	1.1	1.1	1.9[*]	−1.4	1.6	1.6
Valylglycine	Dipeptide[#]	2.1	2.2	3.4[**]	1.6	2.4[*]	2.3[*]
N-Acetylputrescine	Polyamine metabolism	−1.0	−1.0	1.4	1.5	1.3	−1.2
Hydroxy-trimethyllysine	Lysine metabolism	1.0	1.1	1.1	1.6[**]	1.4	1.1

Note: Fold changes for the 14 metabolites that were found to have their levels significantly altered in a multigroup analysis (ANOVA with an FDR of 5%), with pair-wise statistical significance determined by a Tukey HSD post hoc test. The statistical significance of a pathway enrichment analysis is also presented (p-values determined from hypergeometric tests). Doses: 0.5, 50, and 175 mg/kg BW per day of glyphosate (Gly_0.5; Gly_50; Gly_175) or MON 52276 (Mon_0.5; Mon_50; Mon_175). $n = 10$ per group. ANOVA, analysis of variance; FDR, false discovery rate; HSD, honest significant differences. [*], $p < 0.05$; [**], $p < 0.01$; [**], $p < 0.001$; and [#], $p < 0.05$.

treated rats. Fold differences for these compounds generally ranged between 2 and 3. Pathway enrichment analysis also revealed that glyphosate affected the level of dipeptide metabolites (Table 2). Although most differences were very similar between the groups exposed to either glyphosate or MON 52276, additional differences were detected in the latter (compared with controls). The most striking example was lower levels of solanidine and carotenediol, to the extent that they became undetectable at the highest dose of MON 52276.

Host–Microbe Interactions

In order to determine if the differences in serum metabolome composition can be linked to the action of glyphosate on the gut microbiome, or if they are associated with systemic effects, we examined whether levels of metabolites that were altered by glyphosate in the cecum microbiome were also different in the serum metabolome of treated rats. Using a Mantel permutation test of Euclidean distances (employing the method of Spearman), we showed that the composition of the cecum metabolome was correlated to the composition of the serum metabolome (Figure S2). The metabolites 3-dehydroshimate, shikimate, and shikimate 3-phosphate were not detected in serum. In addition, other metabolites differentially detected in the gut of glyphosate-treated rats (2-isopropylmalate, linolenoylcarnitine, glutarate, pimelate, valylglycine, prolylglycine, *N*-acetylputrescine, hydroxy-N6,N6, N6-trimethyllysine) were detected in the serum, but their levels were no different in the serum of glyphosate-treated animals compared with the control group (Tables 2 and 3). Similarly, the levels of these same metabolites were also no different between controls and MON 52276 treatment groups with the exception of glutarate, which was decreased in both serum and cecum samples (Tables 2 and 3).

Serum Metabolomics

Although our analysis showed that the metabolites that had their levels affected by glyphosate or MON 52276 treatment in the cecum were not altered in serum, 33 metabolites had adjusted $p < 0.05$ in the serum metabolomes of glyphosate-treated rats (Table 3; Figure 4). There were significant differences in serum metabolites between vehicle-treated and formulated product MON 52276–treated rats starting at the lowest concentration tested (0.5 mg/kg BW per day), whereas the differences in glyphosate-treated rats were more limited (Table 3). An enrichment analysis revealed that the serum metabolome samples of animals exposed to the treatments reflected differences in nicotinamide, branched-chain amino acid, methionine, cysteine, *S*-adenosyl methionine (SAM), and taurine metabolism (Table 3).

We attempted to quantify shikimic acid levels in serum samples by adapting a published HPLC-SRM-MS–based method (Noh et al. 2020). A comparison of serum and water samples spiked with shikimic acid with a mixture of shikimic acid and albumin revealed that the presence of protein in serum severely compromised the recovery and sensitivity of detection of this compound (Figures S3 and S4). Nevertheless, the estimated limit of detection of shikimic acid in rat serum was $\sim$5–10 ng/mL (Figures S3 and S4). The marked interference of shikimic acid detection by serum proteins in all likelihood explains our inability to detect this compound in the serum of rats exposed to either glyphosate or MON 52276 (Excel Table S14). In summary, our results show that considerable further methodological developments will be needed to quantify shikimic acid levels in serum and which is beyond the scope of the present study.

Shotgun Metagenomics

We then performed a shotgun metagenomics analysis of the cecum microbiome to understand which microorganisms were affected by either glyphosate or MON 52276, or both. No species were detected in a negative extraction control, which was included to ensure that no bacterial contamination was introduced by laboratory reagents and procedures. All the species present in the ZymoBIOMICS Microbial Community Standard control were detected.

Alpha diversity was not different between the experimental groups (Figure 5A; $p = 0.09$). Nonmetric multidimensional scaling of Bray-Curtis distances (beta diversity) showed a separation between the treatment groups and the control group (Figure 5B; $p = 9.9 \times 10^{-5}$). No differences in abundance were detected for the most abundant bacterial phyla (Figure 6A) and species (Figure 6B) present in the cecum microbiome. However, ALDE × 2 analysis revealed that four species present at a low abundance were differentially detected in samples from rats treated with either glyphosate or MON 52276 (FDR < 0.05), compared with those treated with vehicle. *Eggerthella* isolate HGM04355, *Acinetobacter johnsonii*, and *Akkermansia muciniphila* were higher in samples from animals treated with both glyphosate and MON 52276 (Figure 6C–F). Interestingly, *Shinella zoogleoides* abundance was increased in the samples from rats treated with MON 52276 from the lowest dose tested, whereas no difference was observed in samples treated with glyphosate. Because most taxonomy analyses are performed by reference to the abundance of 16S rRNA gene amplicons, we also

Table 3. Serum metabolomics of Sprague-Dawley rats exposed to glyphosate and Roundup MON 52276.

Metabolite	Pathway	Gly_0.5	Gly_50	Gly_175	Mon_0.5	Mon_50	Mon_175
Glyphosate	Chemical[#]	1.0	3.3[***]	19.9[***]	1.0	4.9[***]	16.9[***]
Ectoine	Chemical[#]	1.5	2.1[**]	1.6	1.5	1.0	−1.1
3-Acetylphenol sulfate	Chemical[#]	1.5	2.2[*]	2.8[*]	2.9[***]	3.0[**]	2.1
1-Methylnicotinamide	Nicotinamide metabolism[#]	1.1	−1.1	1.2	1.5	1.9[***]	1.9[***]
Nicotinamide	Nicotinamide metabolism[#]	1.1	−1.0	1.1	1.4[**]	1.2	1.4[**]
3-Methylglutaconate	BCAA metabolism[##]	1.1	−1.0	−1.2	−1.3	−1.5[*]	−1.7[**]
Leucine	BCAA metabolism[##]	−1.1	−1.0	−1.0	1.1	1.1	1.1
Alpha-hydroxyisocaproate	BCAA metabolism[##]	1.2	−1.1	1.2	1.4	1.6	1.3
Isoleucine	BCAA metabolism[##]	−1.1[**]	−1.1	−1.1	−1.0	−1.0	1.0
N-Acetylisoleucine	BCAA metabolism[##]	1.1	1.0	1.1	1.5[*]	1.7[**]	1.6[***]
2,3-Dihydroxy-5-methylthio-4-pentenoate	Sulfur amino acid metabolism[#]	1.1	1.0	−1.1	−1.0	−1.1	−1.2[***]
Taurine	Sulfur amino acid metabolism[#]	1.0	1.0	1.1	1.2[**]	1.1	1.2[**]
Methionine sulfoxide	Sulfur amino acid metabolism[#]	1.0	1.4	1.2	1.0	1.0	−1.2
N-Acetylmethionine sulfoxide	Sulfur amino acid metabolism[#]	1.1	2.3[*]	1.6	1.1	1.7	−1.1
Azelate	Fatty acid, dicarboxylate	1.4	1.9	1.5	1.2	−1.2	−1.1
Glutarate	Fatty acid, dicarboxylate	−1.3	1.1	−1.4	−1.2	−2.1[***]	−1.4
Ribitol	Pentose metabolism[#]	1.1	1.1	1.0	1.2	−1.2	1.0
Ribonate	Pentose metabolism[#]	1.1	1.0	−1.1	1.0	−1.3	1.0
Citrate	TCA cycle	1.0	−1.2[*]	−1.2[*]	−1.2	−1.1	−1.3[**]
Kynurenine	Tryptophan metabolism	1.2	1.1	1.1	1.0	−1.2	−1.1
Xanthurenate	Tryptophan metabolism	1.9	1.4	1.3	1.1	1.4	−1.2
Glutamate	Glutamate metabolism	−1.2	−1.0	−1.1	1.0	−1.3[*]	−1.2
Glycerate	Glycolysis	−1.1	−1.1	−1.2	1.0	−1.4[***]	−1.1
N-Acetylhomocitrulline	Arginine and proline metabolism	1.2	1.4[**]	1.2	1.5[***]	1.4[*]	1.3
Deoxycholate	Secondary bile acid metabolism	−1.4	−1.4	−2.3	−4.8	−14.3	−12.5
4-Hydroxycoumarin	Drug	1.3	1.2	1.3	1.9	2.7[**]	2.3[*]
Alpha-ketoglutarate	TCA cycle	−1.1	−1.1	−1.2	−1.1	−1.4[**]	−1.3
3-Hydroxybutyrate	Ketone bodies	−1.5	−2.1[**]	−1.9[**]	−2.4[***]	−1.9[*]	−1.6
4-Hydroxycinnamate	Food component	1.9	2.7[**]	2.2[*]	1.5	1.2	1.2
Phosphate	Oxidative phosphorylation	1.1	1.1	1.2	1.3	1.7[**]	1.4
N-Acetyl-1-methylhistidine	Histidine metabolism	1.1	1.4	1.3	1.3	1.7[**]	1.2
Guanidinoacetate	Creatine metabolism	−1.1	1.0	−1.2	1.4	−1.2	−1.1
1-Methylguanidine	Guanidine metabolism	1.5	7.3[*]	3.1	3.3	4.9	1.1

Note: Fold changes for the 33 metabolites that were found to have their levels significantly altered in a multigroup analysis (ANOVA with an FDR of 5%), with pair-wise statistical significance determined by a Tukey HSD post hoc test. ANOVA, analysis of variance; BCAA, branched-chain amino acid; FDR, false discovery rate; HSD, honest significant differences; TCA cycle, tricarboxylic acid cycle. The statistical significance of a pathway enrichment analysis is also presented. $n = 10$ per group. Doses: 0.5, 50, and 175 mg/kg BW per day of glyphosate (Gly_0.5; Gly_50; Gly_175) or MON 52276 (Mon_0.5; Mon_50; Mon_175). *p*-values determined from hypergeometric tests). [*], $p < 0.05$; [**], $p < 0.01$; [**], $p < 0.001$; [#], $p < 0.05$, and [##], $p < 0.05$.

studied the taxonomy of sequence reads assigned to 16S rRNA genes. *p*-Values for statistical significance between the experimental groups for the 16S rRNA gene analysis were well correlated to the *p*-values from the shotgun metagenomics analysis ($p = 0.003$) (Figure S5), suggesting that they provide comparable information. However, the analysis of 16S rRNA gene amplicon abundance between the different groups did not provide additional insight into the effects of glyphosate and MON 52276.

We used ShortBRED to quantify the abundance of the EPSPS gene sequences in the cecal metagenomes using a set of 10,809 markers created from the protein sequences of the InterPro family IPR006264. The most significant difference after a Kruskal-Wallis statistical test was an increase in the gene count for the 3-phosphoshikimate 1-carboxyvinyltransferase protein R7B7W1 from *Eggerthella sp. CAG:298*, which was detected at the higher dose (50 mg/kg BW per day) of both glyphosate and MON 52276 (Excel Table S15).

We also performed a functional analysis using the KO assignments provided in the Sprague-Dawley rat gut microbiome gene catalog. A total of eight KO annotations (of 4,028) had their abundance statistically significantly altered by exposure to glyphosate and MON 52276 as compared with the control group at an FDR of 10% (Figure 6G). Interestingly, differences in the abundance of genes assigned to the KO, cysteine-S-conjugate beta-lyase, corroborate the results of the metabolomics, indicating that glyphosate modified levels of cysteine derivatives. Investigation of the relative abundance of bacterial species contributing to cysteine-S-conjugate beta-lyase functional potential in the cecum metabolome was not possible because the taxonomy of these contigs were not assigned in the gene catalog used in the present study.

Growth Inhibition in Vitro

Because previous studies in rats have suggested that the abundance of Lactobacilli in the gut microbiome are affected by glyphosate (Lozano et al. 2018; Mao et al. 2018) but no effects were detected on this taxon in the present shotgun metagenomics analysis, we evaluated the dose- and strain-dependency of glyphosate effects on four different strains of *Lacticaseibacillus rhamnosus* (Figure 7). We observed that glyphosate alone had limited effects on the growth of every bacterial strain, even at a high concentration of 1 g/L.

Given that glyphosate-formulated products are known to exert different effects depending on their co-formulant composition (Clair et al. 2012), we also compared the growth inhibition properties of glyphosate and MON 52276 with those of Roundup GT^+. Interestingly, Roundup GT^+ inhibited bacterial growth at concentrations at which glyphosate and MON 52276 did not present any visible effects (Figure 7).

Discussion

The effects of glyphosate on the gut microbiome are widely debated, with divergent outcomes in studies performed to date. Some studies have indicated that glyphosate can cause alterations in the population of gut microbiota, whereas others have not (Tsiaoussis et al. 2019). One major reason for the discrepancies regarding glyphosate's effects on the gut microbiome may be due

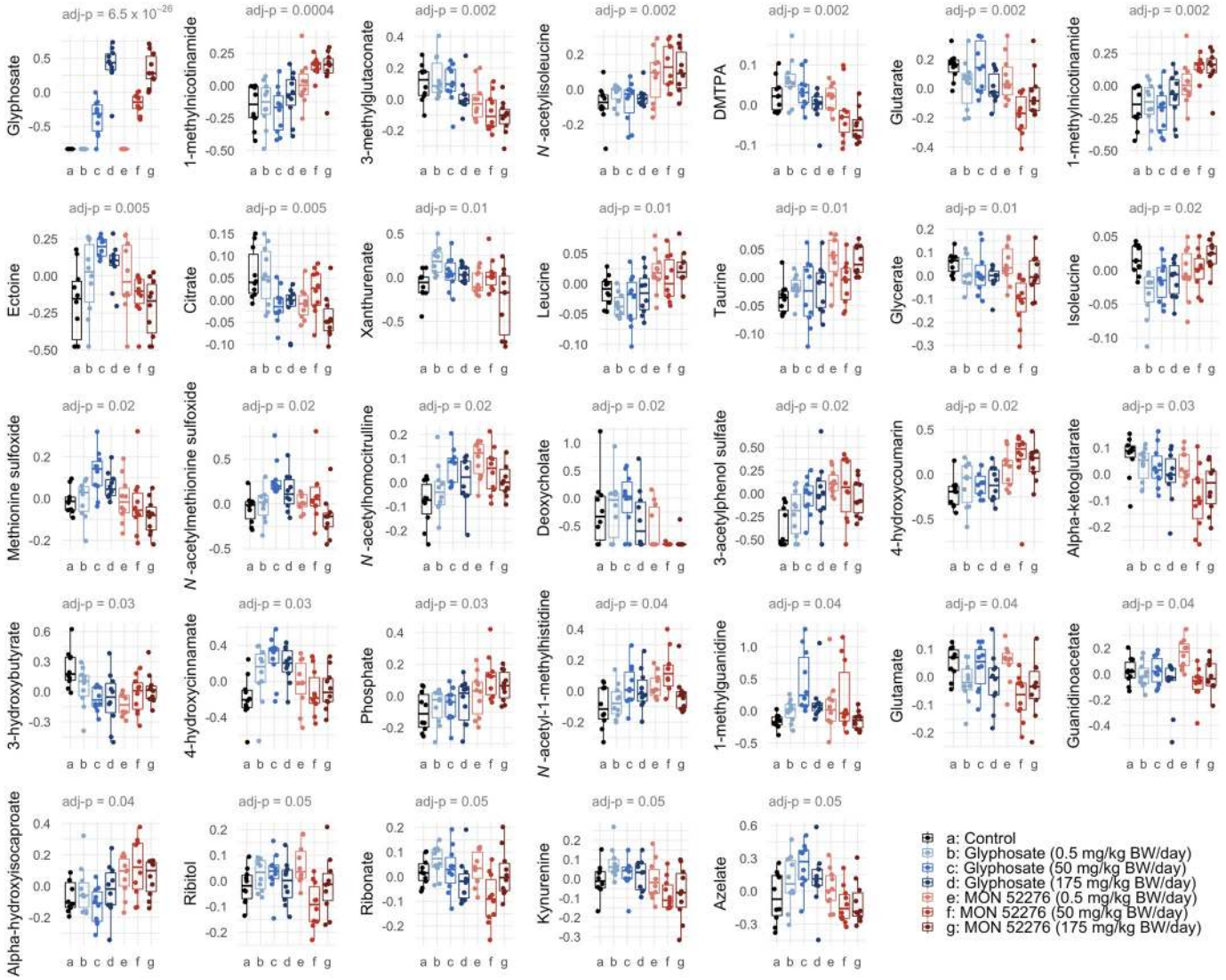

Figure 4. Differences in the level of serum metabolites after exposure to glyphosate or Roundup MON 52276. A total of 33 metabolites had adjusted $p < 0.05$ (*adj-p*) according to an ANOVA adjusted for multiple comparisons with the FDR procedure. Log-transformed abundance values are shown as box plots with the median, two hinges (the 25th and 75th percentiles) and two whiskers extending to the furthest observation ≤ 1.5 times the interquartile range, along with individual values for each metabolite (solid circles). $n = 10$ per group. Note: ANOVA, analysis of variance; BW, body weight; DMTPA, 2,3-dihydroxy-5-methylthio-4-pentenoate; FDR, false discovery rate.

to the lack of studies using advanced molecular profiling analytical techniques. To address this possibility, we used a combination of shotgun-metagenomics and metabolomics to investigate the cecum microbiota of rats exposed to increasing doses of glyphosate and MON 52276. We demonstrated, to our knowledge for the first time, changes in metabolite levels suggesting that glyphosate inhibits the shikimate pathway in the rat cecum microbiome. Although the rat gut microbiome is substantially different from that of humans, we hypothesize that our findings will be of relevance for human physiology because the bacterial species inhabiting the human GI tract have been found to be sensitive to glyphosate-mediated EPSPS inhibition (Tsiaoussis et al. 2019). However, epidemiological studies will be necessary to ascertain whether the doses of glyphosate to which human populations are typically exposed are sufficient to change gut microbiome metabolism.

We found that glyphosate treatment resulted in higher levels of intermediates of the shikimate pathway in the ceca, suggesting inhibition of EPSPS in the cecum microbiome (Figure 3). This mechanism also leads to increases in shikimic acid in soil microorganisms (Aristilde et al. 2017). This might be a general consequence of glyphosate exposure because preharvest glyphosate applications in spring wheat have also resulted in an accumulation of shikimic acid (Malalgoda et al. 2020). Shikimic acid can have multiple biological effects and the toxicological implications of an increase in shikimic acid levels still need to be clarified. On the one hand, shikimate-rich plants such as *Illicium verum* Hook. f. (Chinese star anise) have been traditionally used to treat skin inflammation and stomach aches (Rabelo et al. 2015). Shikimic acid is a plant polyphenolic compound known to protect against oxidative stress (Rabelo et al. 2015) and has antiplatelet and anti-thrombogenic effects (Veach et al. 2016). Other studies have shown that shikimate can cause a dose-dependent activation of the aryl hydrocarbon receptor, a ligand-activated transcription factor with important roles in multiple tissues, including the mucosal immune system (Sridharan et al. 2014). On the other hand, other studies have linked shikimic acid to deleterious health effects. Shikimate has also been implicated as an increased risk factor of gastric and esophageal cancer, found after the consumption of shikimic acid–rich bracken in animals (Evans

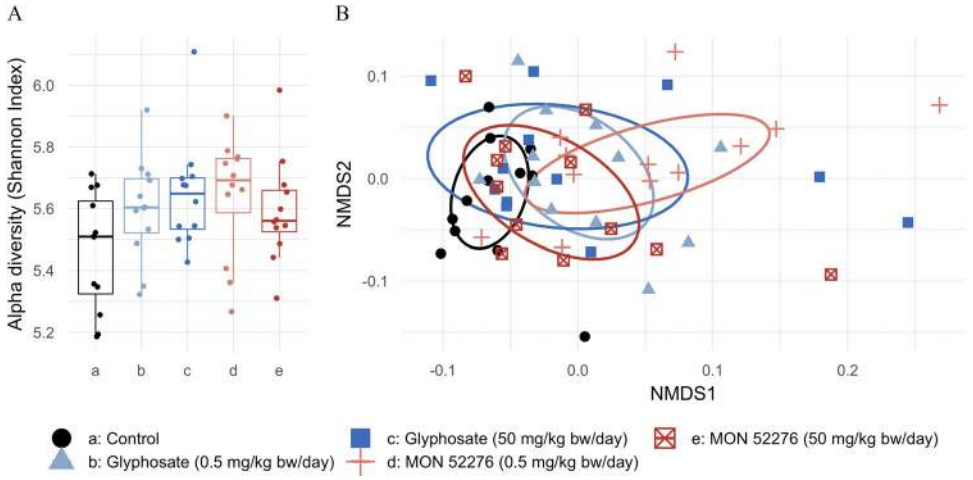

Figure 5. (A) Alpha diversity and (B) beta diversity in the cecum microbiome of rats following 90 d of treatment with glyphosate or Roundup MON 52276. Alpha diversity was calculated from species count data using the diversity function of the R package Vegan. Beta diversity was estimated by calculating pairwise dissimilarities between samples as the Bray-Curtis distance and plotted as a nonmetric multidimensional scaling (NMDS) plot. The statistical significance of this clustering was tested with a 10,000-times permutational multivariate ANOVA test. $n = 12$ per group. Note: ANOVA, analysis of variance; BW, body weight.

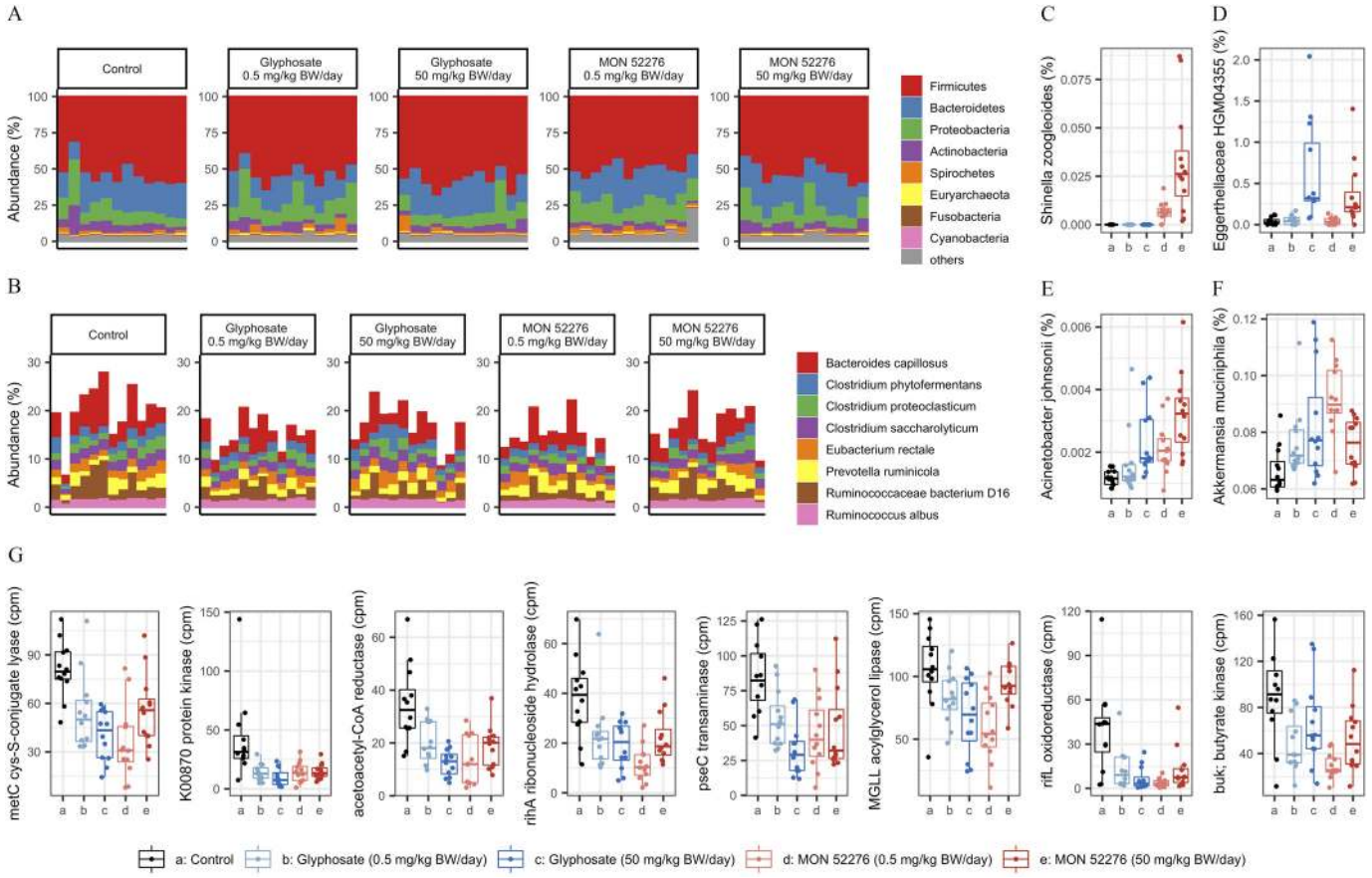

Figure 6. Shotgun metagenomics of rat cecal microbiome composition. Female Sprague-Dawley rats were administered via drinking water with 0.5, 50, and 175 mg/kg BW per day glyphosate and Roundup MON 52276 at the same glyphosate-equivalent dose for 90 d. Cecum content was isolated at the time of sacrifice at the end of the treatment period and processed for metagenomics analysis. The abundance of (A) the most abundant phyla or of (B) the eight species found at an average abundance of >1% is presented. Box plots show the relative abundance for the species (C) *Shinella zoogleoides*, (D) *Acinetobacter johnsonii*, (E) *Eggerthella* isolate HGM04355, and (F) *Akkermansia muciniphila*. (G) Additional box plots display the functional potential assessed by evaluating abundance of KEGG Orthology annotations. Log-transformed abundance values are shown as box plots with the median, two hinges (the 25th and 75th percentiles), and two whiskers extending to the furthest observation ≤1.5 times the interquartile range, along with individual values for each metabolite (solid circles). $n = 12$ per group. Note: BW, body weight; cpm, counts per million; KEGG, Kyoto Encyclopedia of Genes and Genomes.

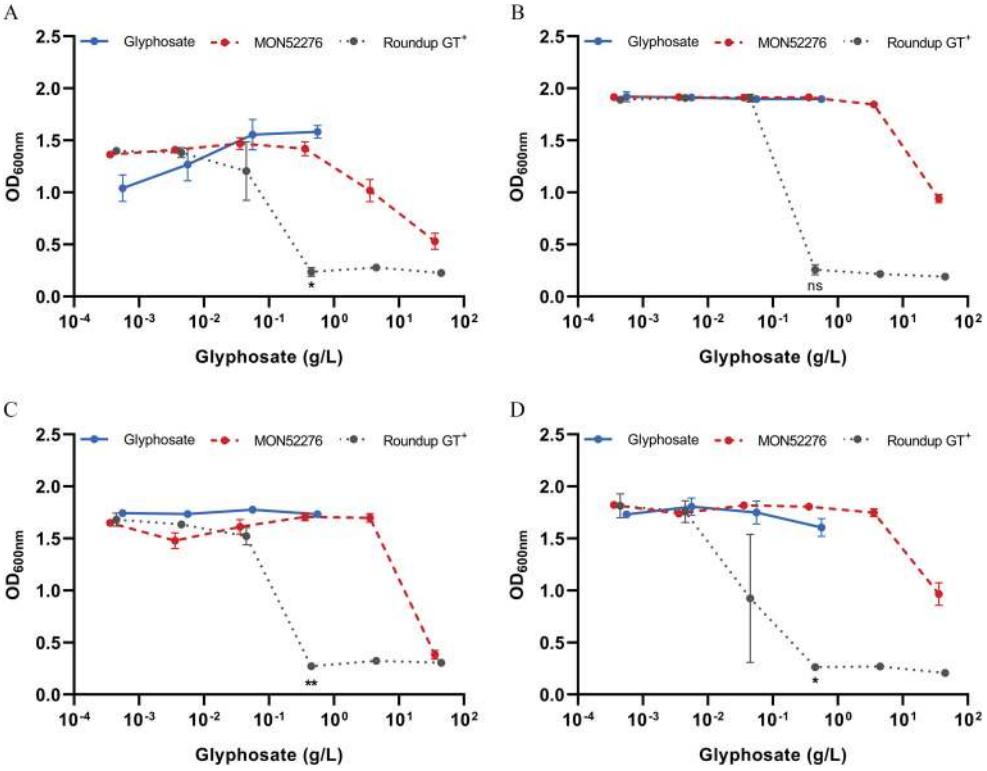

Figure 7. *In vitro* bacterial growth of four different strains of *Lacticaseibacillus rhamnosus* exposed for 48 h to glyphosate alone or to commercial herbicide formulations [Roundup MON 52276, Roundup GT$^+$]. *L. rhamnosus* strains were (A) LB2, (B) LB3, (C) LB5, and (D) LB7. Values are shown as mean ± SD. $n = 3$–4 for each tested concentration. Statistical significance was evaluated using a Kruskal-Wallis test with Dunn's multiple comparison post-test (ns, not significant; $^*p < 0.05$ and $^{**}p < 0.01$). Note: OD, optical density; SD, standard deviation.

and Osman 1974; Wilson et al. 1998). Shikimic acid has been proposed to be a cancer-promoting agent (Jones et al. 1983). A recent study also found that shikimate can stimulate proliferation of a human breast cancer cell line (MCF-7) via activation of NF-κB signaling (Ma and Ning 2019). However, deleterious or beneficial effects are generally two sides of the same coin, especially in the case of polyphenols, which can generate hormetic responses (Calabrese et al. 2010).

The novel mechanism of action of glyphosate on the gut microbiome we describe in the study presented here might be of relevance in the debate on glyphosate's ability to act as a carcinogen (Guyton et al. 2015). Increased levels of shikimic acid caused by glyphosate inhibition of EPSPS may result in shikimate acting as a potential cancer-promoting agent not only in the gut, but also at distant internal organ locations if absorbed. However, further studies should be done, using, for example, germ-free mice to understand if the tumor promoting properties, which have been proposed in some studies with glyphosate (George et al. 2010), can be mediated by an action on the gut microbiome.

Shotgun metagenomics revealed that the composition of the gut microbiome of rats exposed to glyphosate was different from that of those exposed to the vehicle alone (Figures 5 and 6). In general, differences in abundance between individual animals within a group were greater than the effect of test compounds, limiting the conclusions that can be drawn on the biological relevance of the observed statistically significant differences of this gut microbiome functional potential evaluation. Altogether, cecum metabolomics provided more reliable insights to measure functional activity. Although large intragroup variations limit the reliability of the results for a large number of statistically significant differences, some taxonomic groups were affected consistently, and in a dose-dependent manner. The bacterial species *Acinetobacter johnsonii* was found to be more abundant in rats exposed to glyphosate and MON 52276. Although the health relevance of this change is unknown, another member of the *Acinetobacter* genus is known to use glyphosate as a source of phosphorus for growth (Chung et al. 1996). This might indicate that several members of the rat gut microbiome are able to use glyphosate as a source of energy. *Eggerthella* spp. were more abundant in rats exposed to glyphosate and MON 52276. *Eggerthella* spp. are found in the human gut microbiome at a prevalence of approximately 5.5% (Nayfach et al. 2019). Some *Eggerthella* spp. such as *Eggerthella lenta* are potential pathogens commonly associated with infections of the GI tract (Gardiner et al. 2015). The metabolic capabilities of *Eggerthella* spp. have consequences in humans. This genus is known to decrease the efficacy of drugs used to treat cardiac conditions (Haiser et al. 2013). In addition, *Akkermansia muciniphila* was predicted to have its growth affected by glyphosate in a computational modeling of EPSPS sensitivity (Mesnage and Antoniou 2020).

Previous studies have suggested that the bacteria that are most affected by glyphosate in the rat gut microbiome are Lactobacilli (Lozano et al. 2018; Mao et al. 2018; Nielsen et al. 2018). Because the abundance of Lactobacilli was unchanged in our shotgun metagenomics analysis, we further studied the dose- and strain-dependency of glyphosate effects on *L. rhamnosus*. Glyphosate alone had no effect at concentrations that can be expected to be present in the GI tract of rats receiving up to 175 mg/kg BW per day, as in the present study. This suggests that the effects of glyphosate on gut microbiome composition at lower concentrations are restricted to a few taxonomic groups. Further studies will be necessary to clarify the dynamics of gut microbiome compositional alterations induced by glyphosate.

Many studies have reported that commercially formulated pesticide products are more toxic than their active ingredient

alone. This has been shown multiple times for glyphosate-based herbicides (Adam et al. 1997; Manservisi et al. 2019; Mesnage et al. 2013) and also for other classes of pesticides such as insecticides or fungicides (Mesnage et al. 2014). This difference in toxic effects is generally due to the toxicity of surfactants and other compounds that constitute the adjuvant mixture in commercial pesticide formulations (Mesnage et al. 2019), although it cannot be excluded that these surfactants can also potentiate glyphosate penetration in tissues (Anadón et al. 2009). Serum metabolomics suggested that MON 52276 had a greater impact than glyphosate on the serum metabolome, indicating systemic toxic effects. Changes in sulfur amino acid metabolites associated to nicotinamide, branched-chain amino acid, methionine, cysteine, SAM, and taurine metabolism could be an indication of effects on liver function. Nicotinamide is a form of vitamin B3 that can act as a stress signal-mediating compound, released when DNA-strand breakage is caused by oxidative damage (Berglund 1994). Nicotinamide has been shown to protect from hepatic steatosis by increasing the redox potential (Ganji et al. 2014). The higher nicotinamide levels are considered to be a marker of the generation of reactive oxygen species (Schmeisser et al. 2013). In addition, the metabolism of sulfur-containing amino acids has important roles, including protection against oxidative stress (Brosnan and Brosnan 2008). The increase in cysteinylglycine in the cecal microbiome is suggestive that glyphosate also alters cysteine metabolism in the gut microbiome. Interestingly, previous studies have showed that glyphosate exposure in human cell lines influenced cysteine turnover (Hultberg 2007). Collectively, these changes suggest a metabolic adaptation to oxidative stress induced by the exposure to MON 52276 and, to a lesser extent, to glyphosate. This can be connected to the changes in tryptophan derivatives. The conversion of tryptophan to nicotinamide is known to decrease in rats presenting a steatotic liver (Ganji et al. 2014). Our previous findings showed that chronic exposure of rats to an ultra-low dose of Roundup resulted in nonalcoholic fatty liver disease (Mesnage et al. 2015, 2017). Interestingly, the strain of *Eggerthella* spp. found to be increased in abundance by glyphosate in the present study has been reported to be associated with liver cirrhosis in human populations (Nayfach et al. 2019). However, direct investigations of liver tissue will be necessary to corroborate this hypothesis. In addition, longer-term experiments with larger groups of animals will be needed to ascertain if deleterious effects can arise on liver and kidney function. These future experiments could include exposure beginning at a prenatal period of development in order to ascertain lifelong effects (Landrigan and Belpoggi 2018).

Few studies have examined the toxicity of compounds used as pesticide co-formulants on the gut microbiome, with the only comprehensive study published so far suggesting that compounds having emulsifying properties can drive intestinal inflammation by affecting the gut mucosa (Chassaing et al. 2017). The present study suggests that the adjuvant mixture present in MON 52276 had limited effects on the cecum metabolome in comparison with glyphosate, which was the main ingredient responsible for the metabolic changes observed in this study. There were nonetheless taxonomic differences, with *Shinella zoogleoides* found to be increased by exposure to MON 52276 but not glyphosate. The potential roles of *Shinella* spp. in the gut microbiome are still elusive, although it is notable that some have been isolated from various environmental samples, such as activated sludge, and are known to degrade environmental pollutants, including chlorothalonil (Liang et al. 2011) and the alkaloid nicotine (Qiu et al. 2016). We hypothesize that the increase in *Shinella* spp. caused by MON 52276 could affect alkaloid levels in the gut, as suggested by the large decrease in solanidine levels, which was only detected in the MON 52276 treated group. Our *in vitro* comparison of two formulated products also showed that different classes of surfactants used in glyphosate-formulated products can have different toxicity profiles on bacteria (Figure 7), suggesting that results with one formulation should not be generalized to all other GBH products.

Gut microbiome metagenomics and metabolomics can be confounded by a large number of factors that remain largely unidentified (McLaren et al. 2019). The identification of taxonomic differences was limited by different variables, such as the relatively low statistical power provided by the use of 12 animals per group and the incompleteness of the taxonomic classification in gene catalogs, as well as intrinsic factors such as the zero-inflation of metagenomic gene count data (Knight et al. 2012). In addition, different software and pipelines for taxonomic assignment have been shown to provide different results, and there is no gold standard method by which to analyze shotgun metagenomics data sets (Ye et al. 2019). Even the type of instrumentation employed can play a role, with NovaSeq sequencers detecting more DNA sequence diversity within samples than MiSeq sequencers at the exact same sequencing depth (Singer et al. 2019). This could have been amplified in the present study by the housing of 3 rats per cage, given that rats can exchange fecal microorganisms and metabolites by coprophagy (Suckow et al. 2005).

An additional important implication from the present study is that cecal metabolomics was the most effective method to detect glyphosate effects compared with shotgun metagenomics. The amplitude of changes in shikimic acid abundance was very large in comparison with changes in bacterial composition. Gut microbial communities may be resilient to changes in the rat gut given that the nutrients provided by the diet are very abundant and always the same. The *in vitro* evaluation of *Lacticaseibacillus rhamnosus* sensitivity further confirmed that glyphosate alone had limited effects on bacterial growth, even at the highest concentration tested. It is likely that the inhibition of the shikimate pathway does not affect the growth properties of bacteria, which explains why the different studies conducted so far using 16S rRNA gene sequencing did not provide a clear picture of glyphosate effects in the gut. This is corroborated by a study of the soil filamentous fungus *Aspergillus nidulans*, in which Roundup GT^{+} caused alterations in stress response pathways, amino acids, and secondary metabolisms, at a concentration causing no changes in morphology and growth (Mesnage et al. 2020).

In conclusion, the present study demonstrates the power of using multi-omics molecular profiling to reveal changes in the gut microbiome and serum biochemistry following exposure to chemical pollutants that would otherwise be missed using more standard, less comprehensive analytical methods. Employing this approach allowed us to identify glyphosate effects on the rat gut microbiota, namely a marked increase in shikimate and 3-dehydroshikimate reflective of inhibition of EPSPS of the shikimate pathway. In addition, we found higher levels of γ-glutamylglutamine, cysteinylglycine, and valylglycine, suggestive of a response to oxidative stress. Furthermore, serum metabolomics showed that treatment with glyphosate and MON 52276 was associated with altered levels of nicotinamide, branched-chain amino acid, methionine, cysteine, and taurine metabolism, which is also indicative of a response to oxidative stress. Although more studies are needed to understand the health implications of glyphosate inhibition of the shikimate pathway and other metabolic disturbances in the gut microbiome and serum, our findings could be used in the development of biomarkers for epidemiological studies and to understand if glyphosate can have biological effects in human populations.

Acknowledgments

We thank N. Segata and F. Asnicar for assistance in metagenomics data analysis using their preprocessing package and useful discussions on metagenomics analytical pipelines. This work was funded by the Sustainable Food Alliance (USA) and in part by the Sheepdrove Trust (UK).

References

Abraham W, inventor; Monsanto Technology LLC, assignee. Glyphosate formulations and their use for the inhibition of 5-enolpyruvylshikimate-3-phosphate synthase. US patent 7,771,736. 10 August 2010.

Adam A, Marzuki A, Abdul Rahman H, Abdul Aziz M. 1997. The oral and intratracheal toxicities of ROUNDUP and its components to rats. Vet Hum Toxicol 39(3):147–151, PMID: 9167243.

Anadón A, Martínez-Larrañaga MR, Martínez MA, Castellano VJ, Martínez M, Martin MT, et al. 2009. Toxicokinetics of glyphosate and its metabolite aminomethyl phosphonic acid in rats. Toxicol Lett 190(1):91–95, PMID: 19607892, https://doi.org/10.1016/j.toxlet.2009.07.008.

Aristilde L, Reed ML, Wilkes RA, Youngster T, Kukurugya MA, Katz V, et al. 2017. Glyphosate-induced specific and widespread perturbations in the metabolome of soil *Pseudomonas* species. Front Environ Sci 5:34, https://doi.org/10.3389/fenvs.2017.00034.

Barrett KA, McBride MB. 2005. Oxidative degradation of glyphosate and aminomethylphosphonate by manganese oxide. Environ Sci Technol 39(23):9223–9228, PMID: 16382946, https://doi.org/10.1021/es051342d.

Benbrook CM. 2016. Trends in glyphosate herbicide use in the United States and globally. Environ Sci Eur 28(1):3, PMID: 27752438, https://doi.org/10.1186/s12302-016-0070-0.

Berglund T. 1994. Nicotinamide, a missing link in the early stress response in eukaryotic cells: a hypothesis with special reference to oxidative stress in plants. FEBS Lett 351(2):145–149, PMID: 8082753, https://doi.org/10.1016/0014-5793(94)00850-7.

Brewster DW, Warren J, Hopkins WE II. 1991. Metabolism of glyphosate in Sprague-Dawley rats: tissue distribution, identification, and quantitation of glyphosate-derived materials following a single oral dose. Fundam Appl Toxicol 17(1):43–51, PMID: 1916078, https://doi.org/10.1093/toxsci/17.1.43.

Brosnan JT, Brosnan ME. 2008. Glutathione and the sulfur-containing amino acids: an overview. In: *Glutathione and Sulfur Amino Acids in Human Health and Disease*. Masella R, Mazza G, eds. Hoboken, NJ: John Wiley & Sons, 1–18.

Calabrese V, Cornelius C, Trovato A, Cavallaro M, Mancuso C, Di Rienzo L, et al. 2010. The hormetic role of dietary antioxidants in free radical-related diseases. Curr Pharm Des 16(7):877–883, PMID: 20388101, https://doi.org/10.2174/138161210790883615.

Capurso L. 2019. Thirty years of *Lactobacillus rhamnosus* GG: a review. J Clin Gastroenterol 53(suppl 1):S1–S41, PMID: 30741841, https://doi.org/10.1097/MCG.0000000000001170.

Chassaing B, Van de Wiele T, De Bodt J, Marzorati M, Gewirtz AT. 2017. Dietary emulsifiers directly alter human microbiota composition and gene expression ex vivo potentiating intestinal inflammation. Gut 66(8):1414–1427, PMID: 28325746, https://doi.org/10.1136/gutjnl-2016-313099.

Chong J, Soufan O, Li C, Caraus I, Li S, Bourque G, et al. 2018. MetaboAnalyst 4.0: towards more transparent and integrative metabolomics analysis. Nucleic Acids Res 46(W1):W486–W494, PMID: 29762782, https://doi.org/10.1093/nar/gky310.

Chung NJ, Han HJ, Lee HH, Rhie HG, Lee HS. 1996. Degradation of phosphonate herbicide glyphosate by Acinetobacter lwoflii HN401. Mol Cells 6(3):239–245.

Clair E, Linn L, Travert C, Amiel C, Séralini GE, Panoff JM. 2012. Effects of Roundup® and glyphosate on three food microorganisms: *Geotrichum candidum*, *Lactococcus lactis* subsp. *cremoris* and *Lactobacillus delbrueckii* subsp. bulgaricus. Curr Microbiol 64(5):486–491, PMID: 22362186, https://doi.org/10.1007/s00284-012-0098-3.

Coggins JR, Abell C, Evans LB, Frederickson M, Robinson DA, Roszak AW, et al. 2003. Experiences with the shikimate-pathway enzymes as targets for rational drug design. Biochem Soc Trans 31(pt 3):548–552, PMID: 12773154, https://doi.org/10.1042/bst0310548.

DeHaven CD, Evans AM, Dai H, Lawton KA. 2010. Organization of GC/MS and LC/MS metabolomics data into chemical libraries. J Cheminform 2(1):9, PMID: 20955607, https://doi.org/10.1186/1758-2946-2-9.

Ducarmon QR, Zwittink RD, Hornung BVH, van Schaik W, Young VB, Kuijper EJ. 2019. Gut microbiota and colonization resistance against bacterial enteric infection. Microbiol Mol Biol Rev 83(3):e00007-19, PMID: 31167904, https://doi.org/10.1128/MMBR.00007-19.

EFSA (European Food Safety Authority). 2015. Conclusion on the peer review of the pesticide risk assessment of the active substance glyphosate. EFSA J 13(11):4302, https://doi.org/10.2903/j.efsa.2015.4302.

EFSA. 2017. The 2015 European Union report on pesticide residues in food. EFSA J 15(4):4791, https://doi.org/10.2903/j.efsa.2017.4791.

Evans AM, DeHaven CD, Barrett T, Mitchell M, Milgram E. 2009. Integrated, nontargeted ultrahigh performance liquid chromatography/electrospray ionization tandem mass spectrometry platform for the identification and relative quantification of the small-molecule complement of biological systems. Anal Chem 81(16):6656–6667, PMID: 19624122, https://doi.org/10.1021/ac901536h.

Evans IA, Osman MA. 1974. Carcinogenicity of bracken and shikimic acid. Nature 250(464):348–349, PMID: 4211848, https://doi.org/10.1038/250348a0.

Fernandes AD, Macklaim JM, Linn TG, Reid G, Gloor GB. 2013. ANOVA-like differential expression (ALDEx) analysis for mixed population RNA-Seq. PLoS One 8(7):e67019, PMID: 23843979, https://doi.org/10.1371/journal.pone.0067019.

Ford L, Kennedy AD, Goodman KD, Pappan KL, Evans AM, Miller LAD, et al. 2020. Precision of a clinical metabolomics profiling platform for use in the identification of inborn errors of metabolism. J Appl Lab Med 5(2):342–356, PMID: 32445384, https://doi.org/10.1093/jalm/jfz026.

Ganji SH, Kukes GD, Lambrecht N, Kashyap ML, Kamanna VS. 2014. Therapeutic role of niacin in the prevention and regression of hepatic steatosis in rat model of nonalcoholic fatty liver disease. Am J Physiol Gastrointest Liver Physiol 306(4):G320–G327, PMID: 24356885, https://doi.org/10.1152/ajpgi.00181.2013.

Gardiner BJ, Tai AY, Kotsanas D, Francis MJ, Roberts SA, Ballard SA, et al. 2015. Clinical and microbiological characteristics of *Eggerthella lenta* bacteremia. J Clin Microbiol 53(2):626–635, PMID: 25520446, https://doi.org/10.1128/JCM.02926-14.

George J, Prasad S, Mahmood Z, Shukla Y. 2010. Studies on glyphosate-induced carcinogenicity in mouse skin: a proteomic approach. J Proteomics 73(5):951–964, PMID: 20045496, https://doi.org/10.1016/j.jprot.2009.12.008.

Government of Italy. 2014. Decreto Legislativo 4 marzo 2014, n. 26Attuazione della direttiva 2010/63/UE sulla protezione degli animali utilizzati a fini scientifici. (14G00036) (GU Serie Generale n.61 del 14-3-2014). [In Italian.] http://extwprlegs1.fao.org/docs/pdf/ita153404.pdf [accessed 22 December 2020].

Guyton KZ, Loomis D, Grosse Y, El Ghissassi F, Benbrahim-Tallaa L, Guha N, et al. 2015. Carcinogenicity of tetrachlorvinphos, parathion, malathion, diazinon, and glyphosate. Lancet Oncol 16(5):490–491, PMID: 25801782, https://doi.org/10.1016/S1470-2045(15)70134-8.

Haiser HJ, Gootenberg DB, Chatman K, Sirasani G, Balskus EP, Turnbaugh PJ. 2013. Predicting and manipulating cardiac drug inactivation by the human gut bacterium *Eggerthella lenta*. Science 341(6143):295–298, PMID: 23869020, https://doi.org/10.1126/science.1235872.

Henri-Dubernet S, Desmasures N, Guéguen M. 2008. Diversity and dynamics of lactobacilli populations during ripening of RDO Camembert cheese. Can J Microbiol 54(3):218–228, PMID: 18388993, https://doi.org/10.1139/w07-137.

Hove-Jensen B, Zechel DL, Jochimsen B. 2014. Utilization of glyphosate as phosphate source: biochemistry and genetics of bacterial carbon-phosphorus lyase. Microbiol Mol Biol Rev 78(1):176–197, PMID: 24600043, https://doi.org/10.1128/MMBR.00040-13.

Hultberg M. 2007. Cysteine turnover in human cell lines is influenced by glyphosate. Environ Toxicol Pharmacol 24(1):19–22, PMID: 21783784, https://doi.org/10.1016/j.etap.2007.01.002.

Jones RS, Ali M, Ioannides C, Styles JA, Ashby J, Sulej J, et al. 1983. The mutagenic and cell transforming properties of shikimic acid and some of its bacterial and mammalian metabolites. Toxicol Lett 19(1–2):43–50, PMID: 6362076, https://doi.org/10.1016/0378-4274(83)90260-6.

Kaminski J, Gibson MK, Franzosa EA, Segata N, Dantas G, Huttenhower C. 2015. High-specificity targeted functional profiling in microbial communities with ShortBRED. PLoS Comput Biol 11(12):e1004557, PMID: 26682918, https://doi.org/10.1371/journal.pcbi.1004557.

Keegan KP, Glass EM, Meyer F. 2016. MG-RAST, a metagenomics service for analysis of microbial community structure and function. Methods Mol Biol 1399:207–233, PMID: 26791506, https://doi.org/10.1007/978-1-4939-3369-3_13.

Kittle RP, McDermid KJ, Muehlstein L, Balazs GH. 2018. Effects of glyphosate herbicide on the gastrointestinal microflora of Hawaiian green turtles (*Chelonia mydas*) Linnaeus. Mar Pollut Bull 127:170–174, PMID: 29475651, https://doi.org/10.1016/j.marpolbul.2017.11.030.

Knaggs AR. 2001. The biosynthesis of shikimate metabolites. Nat Prod Rep 18(3):334–355, PMID: 11476485, https://doi.org/10.1039/b001717p.

Knight R, Jansson J, Field D, Fierer N, Desai N, Fuhrman JA, et al. 2012. Unlocking the potential of metagenomics through replicated experimental design. Nat Biotechnol 30(6):513–520, PMID: 22678395, https://doi.org/10.1038/nbt.2235.

Koppel N, Maini Rekdal V, Balskus EP. 2017. Chemical transformation of xenobiotics by the human gut microbiota. Science 356(6344):eaag2770, PMID: 28642381, https://doi.org/10.1126/science.aag2770.

Kopylova E, Noé L, Touzet H. 2012. SortMeRNA: fast and accurate filtering of ribosomal RNAs in metatranscriptomic data. Bioinformatics 28(24):3211–3217, PMID: 23071270, https://doi.org/10.1093/bioinformatics/bts611.

Krause JL, Haange SB, Schäpe SS, Engelmann B, Rolle-Kampczyk U, Fritz-Wallace K, et al. 2020. The glyphosate formulation Roundup® LB plus influences the global metabolome of pig gut microbiota *in vitro*. Sci Total Environ 745:140932, PMID: 32731069, https://doi.org/10.1016/j.scitotenv.2020.140932.

Landrigan PJ, Belpoggi F. 2018. The need for independent research on the health effects of glyphosate-based herbicides. Environ Health 17(1):51, PMID: 29843729, https://doi.org/10.1186/s12940-018-0392-z.

Liang B, Wang G, Zhao Y, Chen K, Li S, Jiang J. 2011. Facilitation of bacterial adaptation to chlorothalonil-contaminated sites by horizontal transfer of the chlorothalonil hydrolytic dehalogenase gene. Appl Environ Microbiol 77(12):4268–4272, PMID: 21498744, https://doi.org/10.1128/AEM.02457-10.

Li H, Handsaker B, Wysoker A, Fennell T, Ruan J, Homer N, et al. 2009. The Sequence alignment/map (SAM) format and SAMtools. Bioinformatics 26(16):2078–2079, PMID: 19505943, https://doi.org/10.1093/bioinformatics/btp352.

Lozano VL, Defarge N, Rocque LM, Mesnage R, Hennequin D, Cassier R, et al. 2018. Sex-dependent impact of Roundup on the rat gut microbiome. Toxicol Rep 5:96–107, PMID: 29854581, https://doi.org/10.1016/j.toxrep.2017.12.005.

Ma X, Ning S. 2019. Shikimic acid promotes estrogen receptor(ER)-positive breast cancer cells proliferation via activation of NF-κB signaling. Toxicol Lett 312:65–71, PMID: 31048002, https://doi.org/10.1016/j.toxlet.2019.04.030.

Malalgoda M, Ohm JB, Howatt KA, Green A, Simsek S. 2020. Effects of pre-harvest glyphosate use on protein composition and shikimic acid accumulation in spring wheat. Food Chem 332:127422, PMID: 32623129, https://doi.org/10.1016/j.foodchem.2020.127422.

Manservisi F, Lesseur C, Panzacchi S, Mandrioli D, Falcioni L, Bua L, et al. 2019. The Ramazzini Institute 13-week pilot study glyphosate-based herbicides administered at human-equivalent dose to Sprague Dawley rats: effects on development and endocrine system. Environ Health 18(1):15, PMID: 30857531, https://doi.org/10.1186/s12940-019-0453-y.

Mao Q, Manservisi F, Panzacchi S, Mandrioli D, Menghetti I, Vornoli A, et al. 2018. The Ramazzini Institute 13-week pilot study on glyphosate and Roundup administered at human-equivalent dose to Sprague Dawley rats: effects on the microbiome. Environ Health 17(1):50, PMID: 29843725, https://doi.org/10.1186/s12940-018-0394-x.

McConkey GA, Ittarat I, Meshnick SR, McCutchan TF. 1994. Auxotrophs of *Plasmodium falciparum* dependent on *p*-aminobenzoic acid for growth. Proc Natl Acad Sci USA 91(10):4244–4248, PMID: 8183896, https://doi.org/10.1073/pnas.91.10.4244.

McLaren MR, Willis AD, Callahan BJ. 2019. Consistent and correctable bias in metagenomic sequencing experiments. Elife 8:e46923, PMID: 31502536, https://doi.org/10.7554/eLife.46923.

Mesnage R, Antoniou MN. 2017. Facts and fallacies in the debate on glyphosate toxicity. Front Public Health 5:316, PMID: 29226121, https://doi.org/10.3389/fpubh.2017.00316.

Mesnage R, Antoniou MN. 2020. Computational modelling provides insight into the effects of glyphosate on the shikimate pathway in the human gut microbiome. Curr Res Toxicol 1:25–33, https://doi.org/10.1016/j.crtox.2020.04.001.

Mesnage R, Arno M, Costanzo M, Malatesta M, Seralini GE, Antoniou MN. 2015. Transcriptome profile analysis reflects rat liver and kidney damage following chronic ultra-low dose Roundup exposure. Environ Health 14(1):70, PMID: 26302742, https://doi.org/10.1186/s12940-015-0056-1.

Mesnage R, Benbrook C, Antoniou MN. 2019. Insight into the confusion over surfactant co-formulants in glyphosate-based herbicides. Food Chem Toxicol 128:137–145, PMID: 30951798, https://doi.org/10.1016/j.fct.2019.03.053.

Mesnage R, Bernay B, Seralini GE. 2013. Ethoxylated adjuvants of glyphosate-based herbicides are active principles of human cell toxicity. Toxicology 313(2–3):122–128, PMID: 23000283, https://doi.org/10.1016/j.tox.2012.09.006.

Mesnage R, Defarge N, Spiroux de Vendômois J, Séralini GE. 2014. Major pesticides are more toxic to human cells than their declared active principles. Biomed Res Int 2014:179691, PMID: 24719846, https://doi.org/10.1155/2014/179691.

Mesnage R, Oestreicher N, Poirier F, Nicolas V, Boursier C, Vélot C. 2020. Transcriptome profiling of the fungus *Aspergillus nidulans* exposed to a commercial glyphosate-based herbicide under conditions of apparent herbicide tolerance. Environ Res 182:109116, PMID: 32069763, https://doi.org/10.1016/j.envres.2020.109116.

Mesnage R, Renney G, Séralini GE, Ward M, Antoniou MN. 2017. Multiomics reveal non-alcoholic fatty liver disease in rats following chronic exposure to an ultra-low dose of Roundup herbicide. Sci Rep 7(1):39328, PMID: 28067231, https://doi.org/10.1038/srep39328.

Motta EVS, Raymann K, Moran NA. 2018. Glyphosate perturbs the gut microbiota of honey bees. Proc Natl Acad Sci USA 115(41):10305–10310, PMID: 30249635, https://doi.org/10.1073/pnas.1803880115.

Nayfach S, Shi ZJ, Seshadri R, Pollard KS, Kyrpides NC. 2019. New insights from uncultivated genomes of the global human gut microbiome. Nature 568(7753):505–510, PMID: 30867587, https://doi.org/10.1038/s41586-019-1058-x.

Nielsen LN, Roager HM, Casas ME, Frandsen HL, Gosewinkel U, Bester K, et al. 2018. Glyphosate has limited short-term effects on commensal bacterial community composition in the gut environment due to sufficient aromatic amino acid levels. Environ Pollut 233:364–376, PMID: 29096310, https://doi.org/10.1016/j.envpol.2017.10.016.

Noh K, Back HM, Shin BS, Kang W. 2020. Pharmacokinetics of shikimic acid following intragastric and intravenous administrations in rats. Pharmaceutics 12(9):824, PMID: 32872397, https://doi.org/10.3390/pharmaceutics12090824.

Pan H, Guo R, Zhu J, Wang Q, Ju Y, Xie Y, et al. 2018. A gene catalogue of the Sprague-Dawley rat gut metagenome. Gigascience 7(5):giy055, PMID: 29762673, https://doi.org/10.1093/gigascience/giy055.

Parish T, Stoker NG. 2002. The common aromatic amino acid biosynthesis pathway is essential in *Mycobacterium tuberculosis*. Microbiology (Reading) 148(pt 10):3069–3077, PMID: 12368440, https://doi.org/10.1099/00221287-148-10-3069.

Qiu J, Yang Y, Zhang J, Wang H, Ma Y, He J, et al. 2016. The complete genome sequence of the nicotine-degrading bacterium *Shinella* sp. HZN7. Front Microbiol 7:1348, PMID: 27625640, https://doi.org/10.3389/fmicb.2016.01348.

Rabelo TK, Zeidán-Chuliá F, Caregnato FF, Schnorr CE, Gasparotto J, Serafini MR, et al. 2015. In vitro neuroprotective effect of shikimic acid against hydrogen peroxide-induced oxidative stress. J Mol Neurosci 56(4):956–965, PMID: 25862258, https://doi.org/10.1007/s12031-015-0559-9.

Riede S, Toboldt A, Breves G, Metzner M, Köhler B, Bräunig J, et al. 2016. Investigations on the possible impact of a glyphosate-containing herbicide on ruminal metabolism and bacteria *in vitro* by means of the 'Rumen Simulation Technique'. J Appl Microbiol 121(3):644–656, PMID: 27230806, https://doi.org/10.1111/jam.13190.

Roberts F, Roberts CW, Johnson JJ, Kyle DE, Krell T, Coggins JR, et al. 1998. Evidence for the shikimate pathway in apicomplexan parasites. Nature 393(6687):801–805, PMID: 9655396, https://doi.org/10.1038/31723.

Samsel A, Seneff S. 2013. Glyphosate's suppression of cytochrome P450 enzymes and amino acid biosynthesis by the gut microbiome: pathways to modern diseases. Entropy 15(4):1416–1463, https://doi.org/10.3390/e15041416.

Schmeisser K, Mansfeld J, Kuhlow D, Weimer S, Priebe S, Heiland I, et al. 2013. Role of sirtuins in lifespan regulation is linked to methylation of nicotinamide. Nat Chem Biol 9(11):693–700, PMID: 24077178, https://doi.org/10.1038/nchembio.1352.

Schönbrunn E, Eschenburg S, Shuttleworth WA, Schloss JV, Amrhein N, Evans JN, et al. 2001. Interaction of the herbicide glyphosate with its target enzyme 5-enolpyruvylshikimate 3-phosphate synthase in atomic detail. Proc Natl Acad Sci USA 98(4):1376–1380, PMID: 11171958, https://doi.org/10.1073/pnas.98.4.1376.

Singer GAC, Fahner NA, Barnes JG, McCarthy A, Hajibabaei M. 2019. Comprehensive biodiversity analysis via ultra-deep patterned flow cell technology: a case study of eDNA metabarcoding seawater. Sci Rep 9(1):5991, PMID: 30979963, https://doi.org/10.1038/s41598-019-42455-9.

Sridharan GV, Choi K, Klemashevich C, Wu C, Prabakaran D, Pan LB, et al. 2014. Prediction and quantification of bioactive microbiota metabolites in the mouse gut. Nat Commun 5:5492, PMID: 25411059, https://doi.org/10.1038/ncomms6492.

Suckow MA, Weisbroth SH, Franklin CL. 2005. *The Laboratory Rat*. Boston, MA: Elsevier Science.

Taylor NS, Gavin A, Viant MR. 2018. Metabolomics discovers early-response metabolic biomarkers that can predict chronic reproductive fitness in individual *Daphnia magna*. Metabolites 8(3):42, PMID: 30041468, https://doi.org/10.3390/metabo8030042.

Tsiaoussis J, Antoniou MN, Koliarakis I, Mesnage R, Vardavas CI, Izotov BN, et al. 2019. Effects of single and combined toxic exposures on the gut microbiome: current knowledge and future directions. Toxicol Lett 312:72–97, PMID: 31034867, https://doi.org/10.1016/j.toxlet.2019.04.014.

U.S. EPA (U.S. Environmental Protection Agency). 2002. Glyphosate; pesticide tolerances. a rule by the Environmental Protection Agency on 09/27/2002. Docket No. OPP-2002-0232, FRL-7200-2; Fed Reg 67(188):601934–60950. https://www.govinfo.gov/content/pkg/FR-2002-09-27/pdf/02-24488.pdf [accessed 22 December 2020].

Veach D, Hosking H, Thompson K, Santhakumar AB. 2016. Anti-platelet and anti-thrombogenic effects of shikimic acid in sedentary population. Food Funct 7(8):3609–3616, PMID: 27480079, https://doi.org/10.1039/C6FO00927A.

Wiegand I, Hilpert K, Hancock REW. 2008. Agar and broth dilution methods to determine the minimal inhibitory concentration (MIC) of antimicrobial substances. Nat Protoc 3(2):163–175, PMID: 18274517, https://doi.org/10.1038/nprot.2007.521.

Wilson D, Donaldson LJ, Sepai O. 1998. Should we be frightened of bracken? A review of the evidence. J Epidemiol Community Health 52(12):812–817, PMID: 10396523, https://doi.org/10.1136/jech.52.12.812.

Ye SH, Siddle KJ, Park DJ, Sabeti PC. 2019. Benchmarking metagenomics tools for taxonomic classification. Cell 178(4):779–794, PMID: 31398336, https://doi.org/10.1016/j.cell.2019.07.010.

Zampieri M, Szappanos B, Buchieri MV, Trauner A, Piazza I, Picotti P, et al. 2018. High-throughput metabolomic analysis predicts mode of action of uncharacterized antimicrobial compounds. Sci Transl Med 10(429):eaal3973, PMID: 29467300, https://doi.org/10.1126/scitranslmed.aal3973.

Zhan H, Feng Y, Fan X, Chen S. 2018. Recent advances in glyphosate biodegradation. Appl Microbiol Biotechnol 102(12):5033–5043, PMID: 29705962, https://doi.org/10.1007/s00253-018-9035-0.

Zheng J, Wittouck S, Salvetti E, Franz CMAP, Harris HMB, Mattarelli P, et al. 2020. A taxonomic note on the genus *Lactobacillus*: description of 23 novel genera, emended description of the genus *Lactobacillus* Beijerinck 1901, and union of *Lactobacillaceae* and *Leuconostocaceae*. Int J Syst Evol Microbiol 70(4):2782–2858, PMID: 32293557, https://doi.org/10.1099/ijsem.0.004107.

Zierer J, Jackson MA, Kastenmüller G, Mangino M, Long T, Telenti A, et al. 2018. The fecal metabolome as a functional readout of the gut microbiome. Nat Genet 50(6):790–795, PMID: 29808030, https://doi.org/10.1038/s41588-018-0135-7.